AWARD NUMBER: W81XWH-16-1-0503

TITLE: A Closed-Loop Neural Prosthesis for Restoration of Function After Traumatic Brain Injury

PRINCIPAL INVESTIGATOR: Pedram Mohseni, PhD

CONTRACTING ORGANIZATION: Case Western Reserve University
Cleveland OH 44106

REPORT DATE: September 2017

TYPE OF REPORT: Annual

PREPARED FOR: U.S. Army Medical Research and Materiel Command
Fort Detrick, Maryland 21702-5012

DISTRIBUTION STATEMENT: Approved for Public Release;
Distribution Unlimited

The views, opinions and/or findings contained in this report are those of the author(s) and should not be construed as an official Department of the Army position, policy or decision unless so designated by other documentation.

REPORT DOCUMENTATION PAGE

Form Approved
OMB No. 0704-0188

1. REPORT DATE *(DD-MM-YYYY)* September 2017	2. REPORT TYPE Annual	3. DATES COVERED *(From - To)* 1 Sep 2016 - 31 Aug 2017
4. TITLE AND SUBTITLE A Closed-Loop Neural Prosthesis for Restoration of Function after Traumatic Brain Injury		**5a. CONTRACT NUMBER**
		5b. GRANT NUMBER W81XWH-16-1-0503
		5c. PROGRAM ELEMENT NUMBER
6. AUTHOR(S) Pedram Mohseni, Randolph J. Nudo, David J. Guggenmos email: pxm89@case.edu		**5d. PROJECT NUMBER**
		5e. TASK NUMBER
		5f. WORK UNIT NUMBER
7. PERFORMING ORGANIZATION NAME(S) AND ADDRESS(ES) Case Western Reserve University Univ. of Kansas Medical Center Research 10900 Euclid Avenue 3901 Rainbow Boulevard, MSN 1039 Cleveland, OH 44106 Kansas City, KS 66103		**8. PERFORMING ORGANIZATION REPORT NUMBER**
9. SPONSORING / MONITORING AGENCY NAME(S) AND ADDRESS(ES) U.S. Army Medical Research and Materiel Command Fort Detrick, MD 21702		**10. SPONSOR/MONITOR'S ACRONYM(S)**
		11. SPONSOR/MONITOR'S REPORT NUMBER(S)

12. DISTRIBUTION / AVAILABILITY STATEMENT

Approved for Public Release; distribution unlimited

13. SUPPLEMENTARY NOTES

14. ABSTRACT

Significant progress has been made in developing activity-dependent stimulation (ADS) microdevices for use in both rodent and non-human primate (NHP) models of traumatic brain injury (TBI). A system-on-chip (SoC) for ADS has been successfully fabricated and benchtop tested for electrical functionality, and printed-circuit board (PCB) layouts of rigid-flex substrates for rodent and NHP microdevices have also been devised. Hardware, software, and firmware have also been successfully developed for wireless programming of the ADS SoC from a PC host console via a Bluetooth low energy (BLE) module, a feature that is critical for the NHP microdevices and was previously absent from our rodent microdevices. In parallel, all IACUC and ACURO regulatory approvals for animal testing have been successfully completed, and hardware/software infrastructure have been upgraded and standardized between the collaborating engineering and neurobiology teams to improve compatibility, enhance troubleshooting abilities, and increase recording capabilities.

15. SUBJECT TERMS
Activity-dependent stimulation; Implantable microsystem; Neuroplasticity; Rehabilitation, Traumatic brain injury

16. SECURITY CLASSIFICATION OF:			17. LIMITATION OF ABSTRACT	18. NUMBER OF PAGES	19a. NAME OF RESPONSIBLE PERSON USAMRMC
a. REPORT U	**b. ABSTRACT** U	**c. THIS PAGE** U	UU	55	**19b. TELEPHONE NUMBER** *(include area code)*

Standard Form 298 (Rev. 8-98)
Prescribed by ANSI Std. Z39.18

TABLE OF CONTENTS

1. **INTRODUCTION:** Narrative that briefly (one paragraph) describes the subject, purpose and scope of the research.

> The goal of this project is to use an implantable brain-machine-brain interface (BMBI) to facilitate functional reorganization in spared cortico-cortical connections and enhance behavioral recovery after traumatic brain injury (TBI) in both rodent and non-human primate (NHP) models, which will remarkably advance the neurorehabilitation field at the level of functional neurons and networks.

2. **KEYWORDS:** Provide a brief list of keywords (limit to 20 words).

> Activity-dependent stimulation; Implantable microsystem; Neuroplasticity; Rehabilitation, Traumatic brain injury

3. **ACCOMPLISHMENTS:** The PI is reminded that the recipient organization is required to obtain prior written approval from the awarding agency grants official whenever there are significant changes in the project or its direction.

What were the major goals of the project?
List the major goals of the project as stated in the approved SOW. If the application listed milestones/target dates for important activities or phases of the project, identify these dates and show actual completion dates or the percentage of completion.

> **Major Task 1:** Develop functional microdevices for rodent studies for Aim 1 – Currently underway
> **Major Task 2:** Conduct preclinical efficacy study for optimal time window in ambulatory rats using rodent microdevice – Currently underway
> **Major Task 3:** Develop functional microdevices for rodent studies in Aim 2 – Currently underway
> **Major Task 4:** Conduct preclinical efficacy study for persistence of therapeutic effects in ambulatory rats using rodent microdevice – Expected to start in Q3 of Year 2
> **Major Task 5:** Develop functional microdevices for non-human primate studies – Currently underway
> **Major Task 6:** Conduct preclinical efficacy study in ambulatory non-human primates – Starts in Year 3

What was accomplished under these goals?
For this reporting period describe: 1) major activities; 2) specific objectives; 3) significant results or key outcomes, including major findings, developments, or conclusions (both positive and negative); and/or 4) other achievements. Include a discussion of stated goals not met. Description shall include pertinent data and graphs in sufficient detail to explain any significant results achieved. A succinct description of the methodology used shall be provided. As the project progresses to completion, the emphasis in reporting in this section should shift from reporting activities to reporting accomplishments.

In Year 1, the CWRU team worked on **Major Task 1:** *Develop functional microdevices for rodent studies in Aim 1*, **Major Task 3:** *Develop functional microdevices for rodent studies in Aim 2*, and **Major Task 5:** *Develop functional microdevices for non-human primate [NHP] studies* in Aim 3.

Subtask 1: *Electronics development and testing* (Major Task 1)
Our activity-dependent stimulation (ADS) system-on-chip (SoC) was successfully submitted to The MOSIS Services in April 2017 for fabrication. The fabricated chips (5 packaged for benchtop testing and 35 unpackaged for microdevice construction) were received from MOSIS in July 2017. Upon benchtop testing of the chips, the electronic design was proved to be fully functional.

Subtask 2: *Microdevice assembly and testing* (Major Tasks 1 and 3)
The layout files for the rigid-flex substrate of the rodent microdevice were successfully retrieved and checked against the pin-out diagrams of our new recording/stimulating microelectrode arrays to determine if any changes in the substrate layout were needed. Moreover, several brain-storming sessions were conducted with ProtoConnect LLC to review the step-by-step procedure for assembling the rodent microdevices and take necessary steps to revise the procedure based upon our past experience in assembling these microdevices by ProtoConnect. In parallel, significant work was also performed in collaboration with the neurobiology team at KUMC to successfully upgrade the hardware and software platforms in the extant experimental setup at KUMC for compatibility with new computers and operating systems. This effort was important, because it would allow the KUMC team to proceed with assessing and validating the functionality of 8 existing rodent microdevices at KUMC for performing animal studies (upon receiving the IACUC/ACURO regulatory approvals), while *new* rodent microdevices were being re-developed.

Subtask 1: *Microdevice assembly and testing* (Major Task 5)
Efforts were focused on hardware selection and initial software designs to support Bluetooth low energy (BLE) operations. First, a field survey of multiple BLE modules was conducted based on package size, total power consumption, and other selected electrical features. The Atmel SAMB11 BLE module with ARM M0 Cortex support was chosen due to its small size and the lowest power consumption on the market. The selection of this chipset was crucial as it would significantly impact the lifetime of the NHP microdevice when deployed *in vivo*. Experiments verified that the selected chipset satisfied our allocated current budget of 25µA for an on-board wireless module. Next, we researched universal BLE platforms to create a wireless link to the main PC host console. We decided on Bluegiga's BLED112 due to its versatility and support coding libraries in C#. After both BLED112 and SAMB11 modules were purchased, software and firmware back-ends were developed that successfully established a wireless connection between the PC host console and SAMB11 BLE module for <u>wireless programming of the ADS SoC, a new feature that was not present in previous iterations of our microdevices</u>.

Next, efforts were focused on rigorously testing the reliability and stability of the bidirectional wireless link, covering PC operating system (OS) compatibility, software error recovery, and hardware failure recovery among other items. All tests concluded that the software was compatible with Windows OS and successfully returned all devices to an ultralow-power state in the event of any software or hardware errors. Additionally, the old LabVIEW user interfaces previously used to program our microdevices were re-designed to provide a more reliable user interface coded in C# with graphic support via Microsoft Visual Studio. The new programmer application can be used to generate programming codes for both rodent and NHP microdevices; furthermore, it eliminates all technical issues faced when interfacing with the old LabVIEW software suites.

Finally, progress was made on the hardware design of the NHP microdevice to accommodate the proposed new features. Printed-circuit board (PCB) layouts were developed to assess the overall dimensions of the backpack power unit and the head-mounted unit (containing the ADS SoC), which are the two components of the NHP microdevice. In parallel, work also began on incorporating a programming code in the software to calculate the average stimulation rate in both activity-dependent and open-loop stimulation modes, a critical feature to inform the user in cases of over- or under-stimulation.

In Year 1, the KUMC team worked exclusively on **Major Task 2:** *Conduct preclinical efficacy study for optimal time window in ambulatory rats using rodent microdevice.*

Subtask 1: *Complete institutional IACUC and ACURO review process*
The KUMC IACUC protocol for this project was approved on March 2, 2017. The IACUC-approved protocol was received by ACURO on April 14, 2017 for review. Due to several clarifications that were requested by ACURO, the protocol was ultimately approved on August 23, 2017. Animal approval delays were one of the limitations for completing the project milestones related to Major Task 2.

Subtask 2: *Conduct ambulatory experiments for optimal time window (Aim 1)*
Significant work was performed to re-establish the rodent microdevice testing capabilities at KUMC. Hardware and software infrastructure were upgraded to improve compatibility and increase recording capability. This effort was coordinated with the engineering team at CWRU so that equipment was standardized between CWRU and KUMC in order to improve preparatory testing and troubleshooting abilities. Eight existing rodent microdevices at KUMC were characterized and tested to ensure functionality for future *in vivo* testing. Extensive testing of existing microdevices revealed a mechanical failure mode at the location where the flexible polyimide wings were connected to the microelectrodes' microconnectors. This occurred in 4 out of 8 extant microdevices. As the paucity of extant microdevices would limit the number of animals that we would be able to concurrently implant, a detailed plan was made to provide the KUMC team with an additional 35 microdevices for completion of Major Task 2 (and Major Task 4 in Year 2). Consumables related to the surgical procedures, such as microelectrode arrays, implantation hardware, etc, were also purchased in preparation for the animal procedures, so that they could commence as soon as animal protocols were approved. ACURO approval was received on August 23, 2017, shortly before the end of Year 1 performance period. Six rats were purchased for the initial training phase of the experimental protocol. Neurophysiological data were processed through custom software that also extracted the streaming data, filtered it, and performed semi-automated spike sorting and clustering. An independent investigator then performed visual analyses and error correction. Concurrently, the time stamps of triggering spikes were also extracted from the microdevices. The large datasets needed for the neurophysiological analyses required the installation of a data storage array. Using institutional funds, we installed an 8-bay Synology DiskStation (~25TB) in a Synology Hybrid RAID that is mirrored in a high-availability cluster, and backed up to a 5-bay Synology DiskStation (~21TB). This data storage array will assure the long-term integrity of the resulting neurophysiological data generated from this study. These efforts assured us that the study could proceed as planned, albeit with delays in initiation.

What opportunities for training and professional development has the project provided?
If the project was not intended to provide training and professional development opportunities or there is nothing significant to report during this reporting period, state "Nothing to Report."

Describe opportunities for training and professional development provided to anyone who worked on the project or anyone who was involved in the activities supported by the project. "Training" activities are those in which individuals with advanced professional skills and experience assist others in attaining greater proficiency. Training activities may include, for example, courses or one-on-one work with a mentor. "Professional development" activities result in increased knowledge or skill in one's area of expertise and may include workshops, conferences, seminars, study groups, and individual study. Include participation in conferences, workshops, and seminars not listed under major activities.

Four electrical engineering graduate students at CWRU were trained on a wide range of salient topics, including the development of a wireless link based on a Bluetooth Low Energy (BLE) module for neural interface microdevices, neural signal processing, design of implantable microsystems, and methods of powering/communicating with implantable microsystems. All four students also had professional development opportunities by attending the IEEE International Solid-State Circuits Conference (ISSCC) in February 2017 and IEEE International Symposium on Circuits and Systems (ISCAS) in May 2017.

One research analyst and one postdoctoral fellow at KUMC were trained on creating data management systems and developing data analytic tools, as well as on experimental testing of neural interface microdevices and developing IACUC protocols for regulatory approvals.

How were the results disseminated to communities of interest?
If there is nothing significant to report during this reporting period, state "Nothing to Report."

Describe how the results were disseminated to communities of interest. Include any outreach activities that were undertaken to reach members of communities who are not usually aware of these project activities, for the purpose of enhancing public understanding and increasing interest in learning and careers in science, technology, and the humanities.

Nothing to report.

What do you plan to do during the next reporting period to accomplish the goals?
If this is the final report, state "Nothing to Report."

Describe briefly what you plan to do during the next reporting period to accomplish the goals and objectives.

During the next reporting period we will finalize the design of the rigid-flex substrate and the bill of electronic materials/components to be able to develop fully functional rodent microdevices in support of Major Tasks 1 and 3. We also plan to continue our work on software and hardware development/upgrade for the non-human primate microdevice in support of Major Task 5. Furthermore, we will continue performing Major Task 2 with neurobiology collaborators at KUMC. This includes procuring additional rats, training them on the skilled reach task, and performing the surgical procedures to receive a controlled cortical impact (CCI).

4. **IMPACT:** Describe distinctive contributions, major accomplishments, innovations, successes, or any change in practice or behavior that has come about as a result of the project relative to:

What was the impact on the development of the principal discipline(s) of the project?
If there is nothing significant to report during this reporting period, state "Nothing to Report."

Describe how findings, results, techniques that were developed or extended, or other products from the project made an impact or are likely to make an impact on the base of knowledge, theory, and research in the principal disciplinary field(s) of the project. Summarize using language that an intelligent lay audience can understand (Scientific American style).

Nothing to report.

What was the impact on other disciplines?
If there is nothing significant to report during this reporting period, state "Nothing to Report."

Describe how the findings, results, or techniques that were developed or improved, or other products from the project made an impact or are likely to make an impact on other disciplines.

Nothing to report.

What was the impact on technology transfer?
If there is nothing significant to report during this reporting period, state "Nothing to Report."

Describe ways in which the project made an impact, or is likely to make an impact, on commercial technology or public use, including:
- *transfer of results to entities in government or industry;*
- *instances where the research has led to the initiation of a start-up company; or*
- *adoption of new practices.*

The investigators were awarded a continuation U.S. patent in January 2017. The patent citation appears below. Profs. Mohseni and Nudo have also established a start-up company that in 2017 changed its name from Neuralink Technologies LLC to Neurobond Technologies LLC. The name change was made after trademark rights to the name Neuralink were acquired by Mr. Elon Musk for his newly formed company, Neuralink Corp.

R. J. Nudo, P. Mohseni, D. Guggenmos, and M. Azin, *Methods and Associated Neural Prosthetic Devices for Bridging Brain Areas to Improve Function*, U.S. Patent No. 9,533,150 (Continuation) Awarded on January 3, 2017

What was the impact on society beyond science and technology?
If there is nothing significant to report during this reporting period, state "Nothing to Report."

Describe how results from the project made an impact, or are likely to make an impact, beyond the bounds of science, engineering, and the academic world on areas such as:
- *improving public knowledge, attitudes, skills, and abilities;*
- *changing behavior, practices, decision making, policies (including regulatory policies), or social actions; or*
- *improving social, economic, civic, or environmental conditions.*

Nothing to report.

5. **CHANGES/PROBLEMS:** The PD/PI is reminded that the recipient organization is required to obtain prior written approval from the awarding agency grants official whenever there are significant changes in the project or its direction. If not previously reported in writing, provide the following additional information or state, "Nothing to Report," if applicable:

Changes in approach and reasons for change

Describe any changes in approach during the reporting period and reasons for these changes. Remember that significant changes in objectives and scope require prior approval of the agency.

Nothing to report.

Actual or anticipated problems or delays and actions or plans to resolve them

Describe problems or delays encountered during the reporting period and actions or plans to resolve them.

The CWRU team experienced a delay in submitting their new activity-dependent stimulation (ADS) system-on-chip (SoC) design to The MOSIS Services for fabrication. Nonetheless, the design was successfully submitted for fabrication in April 2017 and received in July 2017 (i.e., in Y1Q4). This was not a major concern, because the KUMC team had not yet obtained full ACURO approval to start the preclinical efficacy studies. The KUMC team experienced an administrative delay in the approval of the ACURO protocol (Major Task 2: Subtask 1), which subsequently delayed the start of Major Task 2: Subtask 2. This was not a major concern either, because the ACURO approval, once obtained, would cover Subtask 1 of Major Tasks 2, 4, and 6 simultaneously, reducing administrative delays further down the road.

Changes that had a significant impact on expenditures

Describe changes during the reporting period that may have had a significant impact on expenditures, for example, delays in hiring staff or favorable developments that enable meeting objectives at less cost than anticipated.

Nothing to report.

Significant changes in use or care of human subjects, vertebrate animals, biohazards, and/or select agents

Describe significant deviations, unexpected outcomes, or changes in approved protocols for the use or care of human subjects, vertebrate animals, biohazards, and/or select agents during the reporting period. If required, were these changes approved by the applicable institution committee (or equivalent) and reported to the agency? Also specify the applicable Institutional Review Board/Institutional Animal Care and Use Committee approval dates.

Significant changes in use or care of human subjects

Not applicable.

Significant changes in use or care of vertebrate animals

Nothing to report.

Significant changes in use of biohazards and/or select agents

Not applicable.

6. **PRODUCTS:** List any products resulting from the project during the reporting period. If there is nothing to report under a particular item, state "Nothing to Report."

- **Publications, conference papers, and presentations**
  Report only the major publication(s) resulting from the work under this award.

  Journal publications. *List peer-reviewed articles or papers appearing in scientific, technical, or professional journals. Identify for each publication: Author(s); title; journal; volume: year; page numbers; status of publication (published; accepted, awaiting publication; submitted, under review; other); acknowledgement of federal support (yes/no).*

  Nothing to report.

  Books or other non-periodical, one-time publications. *Report any book, monograph, dissertation, abstract, or the like published as or in a separate publication, rather than a periodical or series. Include any significant publication in the proceedings of a one-time conference or in the report of a one-time study, commission, or the like. Identify for each one-time publication: author(s); title; editor; title of collection, if applicable; bibliographic information; year; type of publication (e.g., book, thesis or dissertation); status of publication (published; accepted, awaiting publication; submitted, under review; other); acknowledgement of federal support (yes/no).*

  Nothing to report.

  Other publications, conference papers and presentations. *Identify any other publications, conference papers and/or presentations not reported above. Specify the status of the publication as noted above. List presentations made during the last year (international, national, local societies, military meetings, etc.). Use an asterisk (*) if presentation produced a manuscript.*

  Nothing to report.

- **Website(s) or other Internet site(s)**

List the URL for any Internet site(s) that disseminates the results of the research activities. A short description of each site should be provided. It is not necessary to include the publications already specified above in this section.

> Nothing to report.

- **Technologies or techniques**
  Identify technologies or techniques that resulted from the research activities. Describe the technologies or techniques were shared.

> Nothing to report.

- **Inventions, patent applications, and/or licenses**
  Identify inventions, patent applications with date, and/or licenses that have resulted from the research. Submission of this information as part of an interim research performance progress report is not a substitute for any other invention reporting required under the terms and conditions of an award.

> R. J. Nudo, P. Mohseni, D. Guggenmos, and M. Azin, *Methods and Associated Neural Prosthetic Devices for Bridging Brain Areas to Improve Function*, U.S. Patent No. 9,533,150 (Continuation) Awarded on January 3, 2017

- **Other Products**
  Identify any other reportable outcomes that were developed under this project. Reportable outcomes are defined as a research result that is or relates to a product, scientific advance, or research tool that makes a meaningful contribution toward the understanding, prevention, diagnosis, prognosis, treatment and /or rehabilitation of a disease, injury or condition, or to improve the quality of life. Examples include:
  - *data or databases;*
  - *physical collections;*
  - *audio or video products;*
  - *software;*
  - *models;*
  - *educational aids or curricula;*
  - *instruments or equipment;*
  - *research material (e.g., Germplasm; cell lines, DNA probes, animal models);*
  - *clinical interventions;*
  - *new business creation; and*
  - *other*

> Nothing to report.

7. PARTICIPANTS & OTHER COLLABORATING ORGANIZATIONS

What individuals have worked on the project?
Provide the following information for: (1) PDs/PIs; and (2) each person who has worked at least one person month per year on the project during the reporting period, regardless of the source of compensation (a person month equals approximately 160 hours of effort). If information is unchanged from a previous submission, provide the name only and indicate "no change".

Example:

Name:	*Mary Smith*
Project Role:	*Graduate Student*
Researcher Identifier (e.g. ORCID ID):	*1234567*
Nearest person month worked:	*5*
Contribution to Project:	*Ms. Smith has performed work in the area of combined error-control and constrained coding.*
Funding Support:	*The Ford Foundation (Complete only if the funding support is provided from other than this award.)*

Name: Pedram Mohseni
Project Role: PD/PI
Researcher Identifier (e.g. ORCID ID): 0000-0002-2849-4677
Nearest person month worked: 1.9
Contribution to Project: Dr. Mohseni oversaw the project progress related to the development of microdevices at CWRU, and maintained communications with the collaborating team at KUMC.

Name: Randolph Nudo
Project Role: Subaward PI
Researcher Identifier (e.g. ORCID ID): 0000-0002-4674-0907
Nearest person month worked: 0.9
Contribution to Project: Dr. Nudo oversaw the project progress related to the neurobiological studies at KUMC, and maintained communications with the collaborating team at CWRU.

Name: Nicholas Vitale
Project Role: Graduate Student at CWRU
Researcher Identifier (e.g. ORCID ID): -
Nearest person month worked: 12
Contribution to Project: Mr. Vitale has performed work in the area of bidirectional wireless links for the microdevices based on a Bluetooth low energy (BLE) module.

Name: Meysam Azin
Project Role: Independent Contractor for CWRU
Researcher Identifier (e.g. ORCID ID): -
Nearest person month worked: 4
Contribution to Project: Dr. Azin performed work in the area of algorithms and coding as well as verification of experimental setup reliability and stability.

Name:	Reza Erfani
Project Role:	Graduate Student at CWRU
Researcher Identifier (e.g. ORCID ID):	-
Nearest person month worked:	4
Contribution to Project:	Mr. Erfani has performed work in the area of wireless powering of biomedical implants.

Name:	Fatemeh Marefat
Project Role:	Graduate Student at CWRU
Researcher Identifier (e.g. ORCID ID):	-
Nearest person month worked:	4
Contribution to Project:	Ms. Marefat has performed work in the area of integrated circuit development for multichannel biopotential recording.

Name:	Hossein Zamani
Project Role:	Graduate Student at CWRU
Researcher Identifier (e.g. ORCID ID):	-
Nearest person month worked:	4
Contribution to Project:	Mr. Zamani has performed work in the area of neural signal processing for online data compression.

Name:	David Guggenmos
Project Role:	Senior Investigator at KUMC
Researcher Identifier (e.g. ORCID ID):	-
Nearest person month worked:	-
Contribution to Project:	Dr. Guggenmos coordinated the work at KUMC, including preparations for the behavioral and surgical aspects of the neurobiological studies.

Name:	Caleb Dunham
Project Role:	Research Analyst at KUMC
Researcher Identifier (e.g. ORCID ID):	-
Nearest person month worked:	-
Contribution to Project:	Mr. Dunham was responsible for updating and upgrading software and hardware platforms related to the neurophysiological data collection, as well as creating the data management systems and developing data analytic tools.

Name:	Heather Hudson
Project Role:	Post-Doctoral Fellow at KUMC
Researcher Identifier (e.g. ORCID ID):	-
Nearest person month worked:	-
Contribution to Project:	Dr. Hudson performed tasks related to assessing and validating functionality of existing rodent microdevices and assisting with development of the IACUC protocol.

Has there been a change in the active other support of the PD/PI(s) or senior/key personnel since the last reporting period?
If there is nothing significant to report during this reporting period, state "Nothing to Report."

If the active support has changed for the PD/PI(s) or senior/key personnel, then describe what the change has been. Changes may occur, for example, if a previously active grant has closed and/or if a previously pending grant is now active. Annotate this information so it is clear what has changed from the previous submission. Submission of other support information is not necessary for pending changes or for changes in the level of effort for active support reported previously. The awarding agency may require prior written approval if a change in active other support significantly impacts the effort on the project that is the subject of the project report.

Nothing to report.

What other organizations were involved as partners?
If there is nothing significant to report during this reporting period, state "Nothing to Report."

Describe partner organizations – academic institutions, other nonprofits, industrial or commercial firms, state or local governments, schools or school systems, or other organizations (foreign or domestic) – that were involved with the project. Partner organizations may have provided financial or in-kind support, supplied facilities or equipment, collaborated in the research, exchanged personnel, or otherwise contributed.

Provide the following information for each partnership:
Organization Name:
Location of Organization: (if foreign location list country)
Partner's contribution to the project *(identify one or more)*
- *Financial support;*
- *In-kind support (e.g., partner makes software, computers, equipment, etc, available to project staff);*
- *Facilities (e.g., project staff use the partner's facilities for project activities);*
- *Collaboration (e.g., partner's staff work with project staff on the project);*
- *Personnel exchanges (e.g., project staff and/or partner's staff use each other's facilities, work at each other's site); and*
- *Other*

Organization Name: University of Kansas Medical Center
Location of Organization: Kansas City, KS, USA
Partner's contribution to the project: Collaboration

8. **SPECIAL REPORTING REQUIREMENTS**

COLLABORATIVE AWARDS: For collaborative awards, independent reports are required from BOTH the Initiating Principal Investigator (PI) and the Collaborating/Partnering PI. A duplicative report is acceptable; however, tasks shall be clearly marked with the responsible PI and research site. A report shall be submitted to **https://ers.amedd.army.mil** for each unique award.

QUAD CHARTS: b/a

9. APPENDICES: attached

(12) **United States Patent**
Nudo et al.

(10) **Patent No.:** **US 9,533,150 B2**
(45) **Date of Patent:** *Jan. 3, 2017

(54) **METHODS AND ASSOCIATED NEURAL PROSTHETIC DEVICES FOR BRIDGING BRAIN AREAS TO IMPROVE FUNCTION**

(71) Applicants: **UNIVERSITY OF KANSAS**, Lawrence, KS (US); **CASE WESTERN RESERVE UNIVERSITY**, Cleveland, OH (US)

(72) Inventors: **Randolph J. Nudo**, Overland Park, KS (US); **Pedram Mohseni**, Shaker Heights, OH (US); **David Guggenmos**, Kansas City, KS (US); **Meysam Azin**, San Diego, CA (US)

(73) Assignees: **UNIVERSITY OF KANSAS**, Lawrence, KS (US); **CASE WESTERN RESERVE UNIVERSITY**, Cleveland, OH (US)

(*) Notice: Subject to any disclaimer, the term of this patent is extended or adjusted under 35 U.S.C. 154(b) by 0 days.

This patent is subject to a terminal disclaimer.

(21) Appl. No.: **14/630,375**

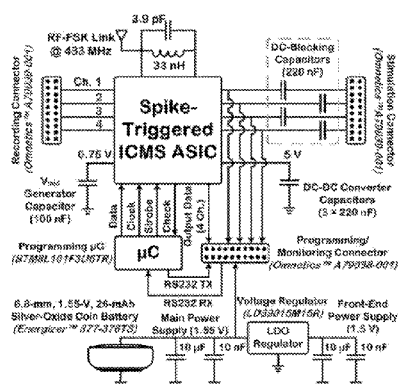(22) Filed: **Feb. 24, 2015**

(65) **Prior Publication Data**

US 2015/0231397 A1 Aug. 20, 2015

Related U.S. Application Data

(63) Continuation of application No. 13/523,597, filed on Jun. 14, 2012, now Pat. No. 9,008,780.
(Continued)

(51) **Int. Cl.**
A61N 1/05 (2006.01)
A61N 1/36 (2006.01)
(Continued)

(52) **U.S. Cl.**
CPC *A61N 1/36103* (2013.01); *A61B 5/6868* (2013.01); *A61N 1/0531* (2013.01); *A61N 1/36139* (2013.01); *A61B 5/04001* (2013.01)

(58) **Field of Classification Search**
CPC .. A61N 1/0529; A61N 1/0531; A61N 1/0536; A61N 1/3605; A61N 1/36103; A61N 1/37205; A61B 5/04001; A61B 5/6868
See application file for complete search history.

(56) **References Cited**

U.S. PATENT DOCUMENTS

3,850,161 A 11/1974 Liss
3,955,560 A 5/1976 Stein et al.
(Continued)

OTHER PUBLICATIONS

Koivuniemi, A.S.; Otto, K.J., "Asymmetric Versus Symmetric Pulses for Cortical Microstimulation," in Neural Systems and Rehabilitation Engineering, IEEE Transactions on , vol. 19, No. 5, pp. 468-476, Oct. 2011.*
(Continued)

Primary Examiner — Eugene T Wu
(74) *Attorney, Agent, or Firm* — Workman Nydegger

(57) **ABSTRACT**

Methods for bridging brain sites between which there is substantially no effective communication, and associated neural prosthetic devices, are provided. A neural spike in a first neural site in a subject is detected, and a stimulus to a second neural site in the subject is delivered within a defined period of time after the detection of the neural spike, wherein there is substantially no effective communication between the first and second neural sites. The method forms an artificial bridge between the two neural sites, and establishes lasting communication between the two sites. The present disclosure provides, among other things, a neural prosthetic device comprising an integrated circuit that comprises a recording front-end comprising a plurality of record-
(Continued)
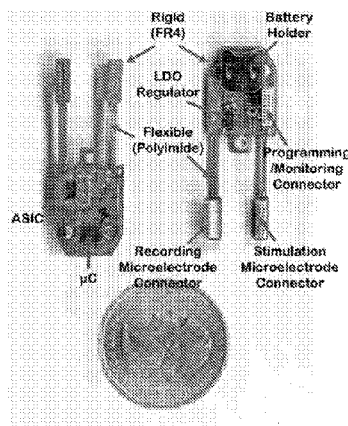
ing channels; a processor unit; and a stimulus delivering back-end comprising a plurality of stimulation channels.

20 Claims, 22 Drawing Sheets

Related U.S. Application Data

(60) Provisional application No. 61/543,593, filed on Oct. 5, 2011.

(51) **Int. Cl.**
  A61B 5/00   (2006.01)
  A61B 5/04   (2006.01)

(56)   **References Cited**

U.S. PATENT DOCUMENTS

4,632,116	A	12/1986	Rosen et al.
5,030,225	A	7/1991	Aebischer et al.
5,048,522	A	9/1991	Petrofsky
7,010,351	B2	3/2006	Firlik
7,092,763	B1	8/2006	Griffith
7,991,465	B2	8/2011	Bartic et al.
9,008,780	B2	4/2015	Nudo et al.
2005/0119703	A1	6/2005	DiLorenzo
2005/0137648	A1	6/2005	Cosendai et al.
2005/0203366	A1	9/2005	Donoghue et al.
2005/0240242	A1	10/2005	DiLorenzo
2005/0251221	A1	11/2005	Zdravkovic
2006/0009814	A1	1/2006	Schulman
2006/0173259	A1	8/2006	Flaherty et al.
2006/0200206	A1	9/2006	Firlik et al.
2007/0032738	A1	2/2007	Flaherty et al.
2007/0032834	A1	2/2007	Gliner et al.
2007/0043401	A1	2/2007	John
2007/0067003	A1	3/2007	Sanchez et al.
2007/0112393	A1	5/2007	Gliner
2007/0179584	A1	8/2007	Gliner
2007/0282389	A1	12/2007	Moxon et al.
2009/0105786	A1	4/2009	Fetz et al.
2009/0112286	A1	4/2009	Wang et al.
2011/0009922	A1	1/2011	Assaf et al.
2012/0232631	A1	9/2012	Frewin et al.

OTHER PUBLICATIONS

Mavoori et al. "An autonomous implantable computer for neural recording and stimulation in unrestrained primates." Journal of Neuroscience Methods, vol. 148, Issue 1, Oct. 15, 2005, pp. 71-77.*
Mavoori, et al. "An Autonomous implantable computer for neutral recording and stimulation in unrestrained primates." *Journal of Neuroscience Methods* 148 (2005), p. 71-77.
M. Azin, D. J. Guggenmos, S. Barbay, R. J. Nudo, and P. Mohseni, "A battery-powered activity-dependent intracortical microstimulation IC for brain-machine-brain interface," *IEEE J. Solid-State Circuits*, vol. 46, No. 4, Apr. 2011, *In Press*.
M. Azin, D. J. Guggenmos, S. Barbay, R. J. Nudo, and P. Mohseni, An activity-dependent brain microstimulation SoC with integrated 23 nV/rtHz neural recording front-end.
M. Azin and P. Mohseni, "A high-output-impedance current microstimulator for anatomical rewiring of cortical circuitry," in Proc. IEEE Int. Symp. Circuits and Systems (ISCAS'08), Seattle, WA, May 18-21, 2008, pp. 2502-2505.
Azin, M.; Guggenos, J.J.; Barbay, S.; Nudo, R.J.; Mohseni, P., "A Miniaturized System for Spike-Triggered Intracortical Microstimuation in an Ambulatory Rat," Biomedical Engineering, IEEE Transactions on, vol. 58, No. 9, pp. 2589, 2597, Sep. 2011.
A. Jackson, C. T. Moritz, J. Mavoori, T. H. Lucas, and E. E. Fetz, "The neurochip BCI: Towards a neural prosthesis for upper limb function," *IEEE Trans. Neural Syst. Rehab. Eng.*, vol. 14, No. 2, pp. 187-190, Jun. 2006.

S. Venkatraman, K. Elkabany, J. D. Long, Y. Yao, and J. M. Carmena, "A system for neural recording and closed-loop intracortical microstimulation in awake rodents," *IEEE Trans. Biomed. Eng.*, vol. 56, No. 1, pp. 15-22, Jan. 2009.
Muller, Jan. "Sub-millisecond closed-loop feedback stimulation between arbitrary sets of individual neurons." *Frontiers in Neural Circuits*, vol. 6, Art 121, Jan. 2013.
Zanos, S.; Richardson, A.G.: Shupe, L.; Miles, F.P.; Fetz, E.E., "The Neurochip-2: An Autonomous Head-Fixed Computer for Recording and Stimulating in Freely Behaving Monkeys," Neural Systems and Rehabilitation Engineering, IEEE Transactions on, vol. 19, No. 4, pp. 427, 435, Aug. 2011.
Stanslaski, S., et al., "Design and Validation of a Fully Implantable, Chronic, Closed-Loop Neuromodulation Device With Concurrent Sensing and Stimulation," *IEEE Transactions on Neural Systems and Rehabilitation Engineering*, vol. 20, No. 4, Jul. 2012, pp. 410-421.
M. M. Ahmadi, "A new modeling and optimization of gain-boosted cascode amplifier for high-speed and low-voltage applications," IEEE Trans. Circuits Syst. II, vol. 53, No. 3, pp. 169173, Mar. 2006.
A. T. Avestruz, W. Santa, D. Carlson, R. Jensen, S. Stanslaski, A. Helfenstine, and T. Denison, "A 5 11W/channel spectral analysis IC for chronic bidirectional brain-machine interfaces," *IEEE J. Solid-State Circuits*, vol. 43, No. 12, pp. 3006-3024, Dec. 2008.
T. W. Berger et al., "Restoring lost cognitive function: Hippocampalcortical neural prostheses," *IEEE Eng. Med. Biol. Mag.*, vol. 24, No. 5, pp. 30-44, Sep./Oct. 2005.
P. K. Campbell, K. E. Jones, R. J. Huber, K. W. Horch, and R. A. Normann, "A silicon-based, three-dimensional neural interface: Manufacturing process for an intracortical electrode array," *IEEE Trans. Biomed. Eng.*, vol. 38, pp. 758-767,1991.
M. S. Chae, Z. Yang, M. R. Yuce, L. Hoang, and W. Liu, "A 128-channel 6-mW wireless neural recording IC with spike feature extraction and UWB transmitter," *IEEE Trans. Neural Syst. Rehab. Eng.*, vol. 17, No. 4, pp. 312-321, Aug. 2009.
T. Chen, K. Chen, Z. Yang, K. Cockerham, and W. Liu, "A biomedical multiprocessor SoC for closed-loop neuroprosthetic applications," in *IEEE Int. Solid State Circuits Conference (ISSCC'09) Dig. Tech. Papers*, San Francisco, CA, Feb. 8-12, 2009, pp. 434-435.
T. G. Constandinou, J. Georgiou, and C. Toumazou, "A partial-current-steering biphasic stimulation driver for vestibular prostheses," *IEEE Trans. Biomed. Circuits Syst.*, vol. 2, No. 2, pp. 106-113, Jun. 2008.
T. Denison, K. Consoer, W. Santa, A.-T. Avestruz, J. Cooley, and A. Kelly, "A 2 ☐ W100 nV/rtHz chopper-stabilized instrumentation amplifier for chronic measurement of neural field potentials," IEEE J. Solid-State Circuits, vol. 42, No. 12, pp. 2934-2945, Dec. 2007.
X. J. Feng, B. Greenwald, H. Rabitz, E. Shea-Brown, and B. Kosut, "Toward closed-loop optimization of deep brain stimulation for Parkinson's disease: Concepts and lessons from a computational model," *J. Neural Eng.*, vol. 4, pp. L14-21,2007.
M. Ghovanloo and K. Najafi, "A compact large-voltage-compliance high-outputimpedance programmable current source for implantable microstimulators," *IEEE Trans. Biomed. Eng.*, vol. 52, No. 1, pp. 97-105, Jan. 2005.
R. R. Harrison and C. Charles, "A low-power low-noise CMOS amplifier for neural recording applications," *IEEE J. Solid-State Circuits*, vol. 38, No. 6, pp. 958-965, Jun. 2003.
L. R. Hochberg, M. D. Serruya, G. M. Friehs, J. A. Mukand, M. Saleh, A. FL Caplan, A. Branner, D. Chen, R. D. Penn, and J. P. Donoghue, "Neuronal ensemble control of prosthetic devices by a human with tetraplegia," *Nature*, vol. 442, pp. 164-171, Jul. 2006.
A. Jackson, J. Mavoori, and E. E. Fetz, "Long-term motor cortex plasticity induced by an electronic neural implant," *Nature*, vol. 444, pp. 56-60, Nov. 2006.
A. Keller and H. Asanuma, "Synaptic relationships involving local axon collaterals of pyramidal neurons in the cat motor cortex," *J. Comp. Neurol.*, vol. 336, pp. 229-242,1993.
J. Lee, H. G. Rhew, D. R. Kipke, and M. P. Flynn, "A 64-channel programmable closed-loop neurostimulator with 8-channel neural amplifier and logarithmic ADC," *IEEE J. Solid-State Circuits*, vol. 45, No. 9, pp. 1935-1945, Sep. 2010.

(56)　　　　**References Cited**

OTHER PUBLICATIONS

X. Liu, A. Demosthenous, and N. Donaldson, "An integrated implantable stimulator that is fail-safe without off-chip blocking capacitors," *IEEE Trans. Biomed. Circuits Syst*., vol. 2, No. 3, pp. 231-244, Sep. 2008.

D. J. McFarland and J. R. Wolpaw, "Brain-computer interface operation of robotic and prosthetic devices," *Computer*, vol. 41, No. 10, pp. 52-56, Oct. 2008.

M. Mollazadeh, K. Murari, G. Cauwenberghs, and N. Thakor, "Micropower CMOSintegrated low-noise amplification, filtering, and digitization of multimodal neuropotentials," *IEEE Trans. Biomed. Circuits Syst*., vol. 3, No. 1, pp. 1-10, Feb. 2009.

C. T. Moritz, S. I. Perlmutter, and E. E. Fetz, "Direct control of paralyzed muscles by cortical neurons," *Nature*, vol. 456, pp. 639-643,2008.

M. A. L. Nicolelis, A. A. Ghazanfar, B. M. Faggin, S. Votaw, and L. M. 0. Oliveira, "Reconstructing the Engram: Simultaneous, multisite, many single neuron recordings," *Neuron*, vol. 18, pp. 529-537, Apr. 1997.

M. Nishibe, S. Barbay, D. Guggenmos, and R. J. Nudo, "Reorganization of motor cortex after controlled cortical impact in rats and implications for functional recovery," *J. Neurotrauma*, vol. 27, pp. 2221-2232, Dec. 2010.

M. Ortmanns, A. Rocke, M. Gehrke, and H. J. Tiedtke, "A 232-channel epiretinal stimulator ASIC," *IEEE J. Solid-State Circuits*, vol. 42, No. 12, pp. 2946-2959, Dec. 2007.

J. P. Rauschecker and R. V. Shannon, "Sending sound to the brain," *Science*, vol. 295, No. 5557, pp. 1025-1029, Feb. 2002.

F. Shahrokhi, K. Abdelhalim, D. Serletis, P. L. Carlen, and R. Genov, "The 128-channel fully differential integrated neural recording and stimulation interface," *IEEE Trans. Biomed. Circuits Syst*., vol. 4, No. 3, pp. 149-161, Jun. 2010.

J. J. Sit and R. Sarpeshkar, "A low-power blocking-capacitor-free charge-balanced electrode-stimulator chip with less than 6 nA dc error for 1-mA full-scale stimulation," *IEEE Trans. Biomed. Circuits Syst*., vol. 1, No. 3, pp. 172-183, Sep. 2007.

A. M. Sodagar, G. E. Perlin, Y. Yao, K. Najafi, and K. D. Wise, "An implantable 64-channel wireless microsystem for single-unit neural recording," *IEEE J. Solid-State Circuits*, vol. 44, No. 9, pp. 2591-2604, Sep. 2009.

K. Sooksood, T. Stieglitz, and M. Ortmanns, "An active approach for charge balancing in functional electrical stimulation," *IEEE Trans. Biomed. Circuits Syst*., vol. 4, No. 3, pp. 162-170, Jun. 2010.

Y. Tsividis, *Operation and Modeling of the MOS Transistor*, 2nd ed. New York, NY: Oxford Univ. Press, 1999.

B. K. Thurgood, D. J. Warren, N. M. Ledbetter, G. A. Clark, and R. R. Harrison, "A wireless integrated circuit for 100-channel charge-balanced neural stimulation," *IEEE Trans. Biomed. Circuits Syst*., vol. 3, No. 6, pp. 405-414, Dec. 2009.

M. Velliste, S. Perel, M. C. Spalding, A. S. Whitford, and A. B. Schwartz, "Cortical control of a prosthetic arm for self-feeding," *Nature*, vol. 453, pp. 1098-1101, Jun. 2008.

Ghez, Claude, Voluntary Movement, Principles of Neural Science. Kandel, et al (Eds.), Sep. 2001, pp. 609-613, Elsevier, New York, New York.

U.S. Appl. No. 13/523,597, Jun. 11, 2013, Office Action.

U.S. Appl. No. 13/523,597, Jan. 15, 2014, Office Action.

U.S. Appl. No. 13/523,597, Aug. 29, 2014, Office Action.

U.S. Appl. No. 13/523,597, Nov. 24, 2014, Notice of Allowance.
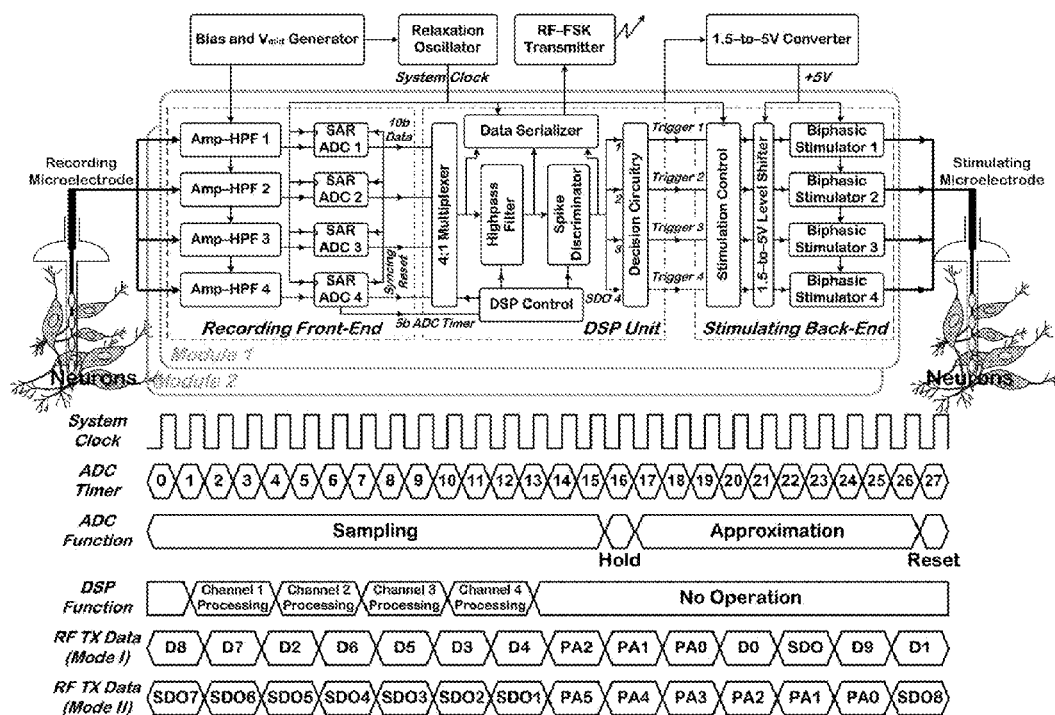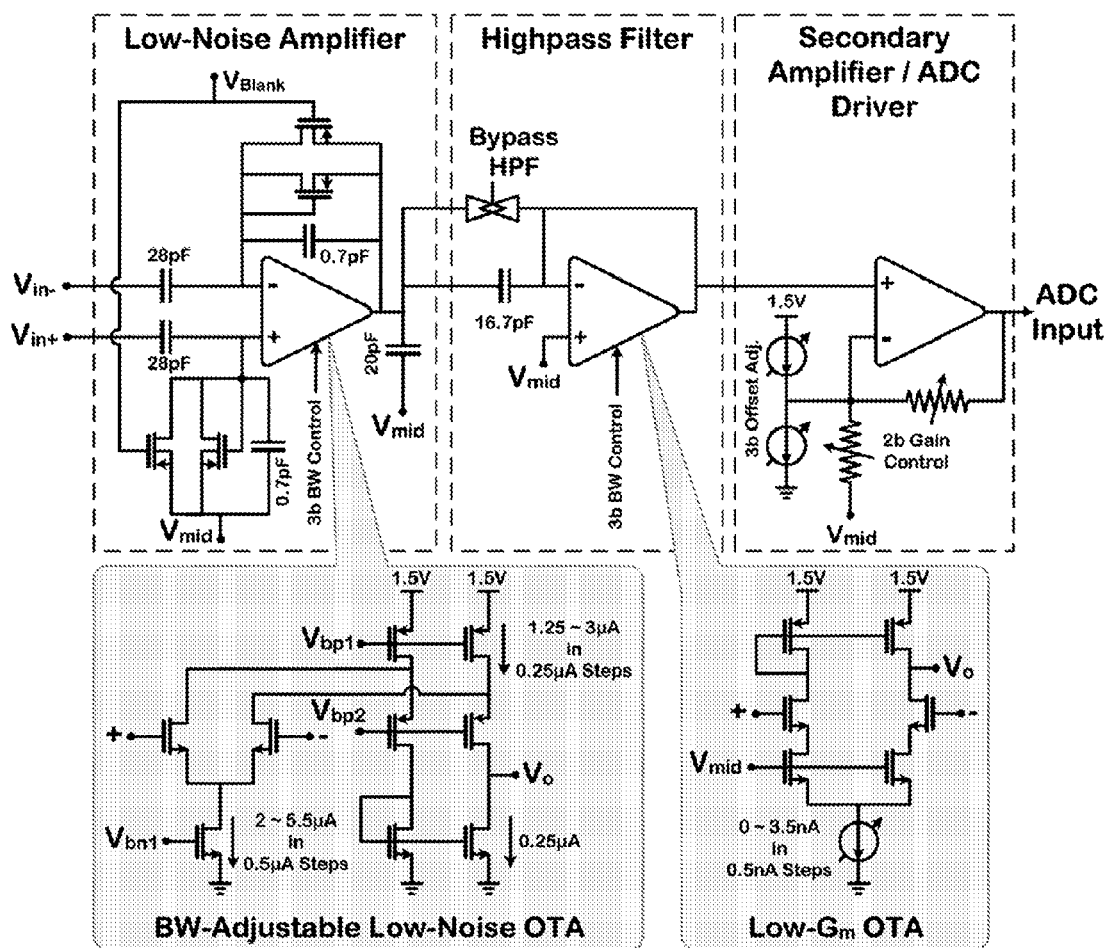
* cited by examiner

Figure 1

Figure 2

Low-Noise Amplifier

Highpass Filter

Secondary Amplifier / ADC Driver

V_{Blank}

Bypass HPF

28pF

0.7pF

V_{in-}

V_{in+}

28pF

20pF

16.7pF

V_{mid}

0.7pF

3b BW Control

V_{mid}

3b BW Control

1.5V

3b Offset Adj.

2b Gain Control

V_{mid}

ADC Input

1.5V   1.5V

V_{bp1} 1.25 ~ 3µA in 0.25µA Steps

V_{bp2}

+   −

V_o

V_{bn1} 2 ~ 5.5µA in 0.5µA Steps

0.25µA

BW-Adjustable Low-Noise OTA

1.5V   1.5V

V_o

+   −

V_{mid}

0 ~ 3.5nA in 0.5nA Steps

Low-G_m OTA

Figure 3

Figure 4

Figure 5

Figures 6A-6D

(a)

(b)

(c)

(d)

Figures 7A-7D

(a)

(b)

(c)
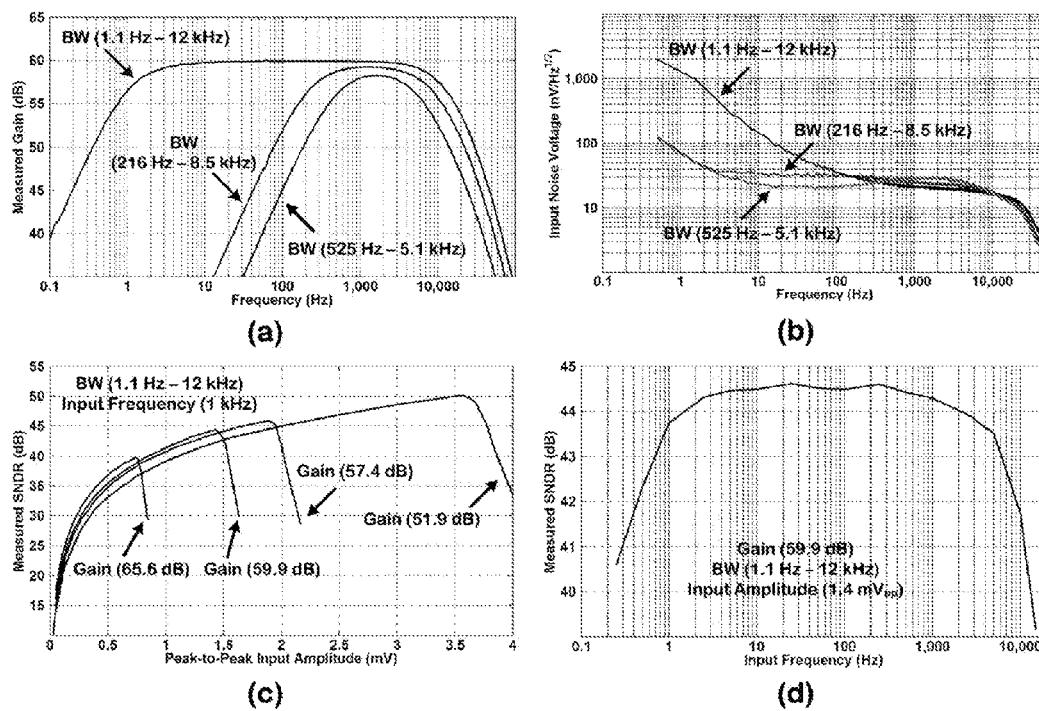
(d)

Figure 8

Figure 9

Figure 10

Figure 11

Figure 12

SoC Area Breakdown
(I/O pads not included)

SoC Power Breakdown
(RF TX not included)
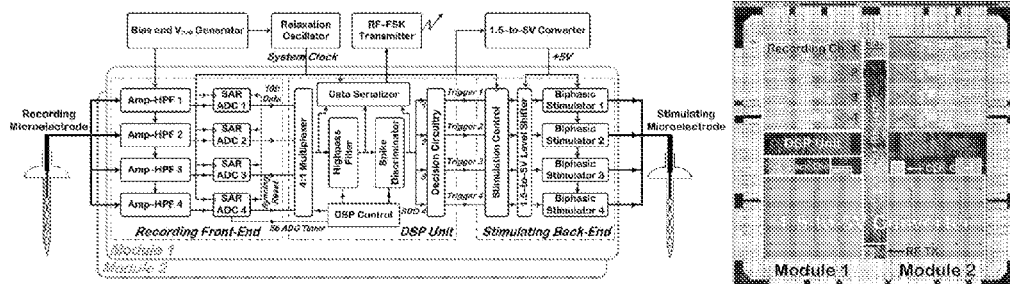
Figure 13

Figure 14

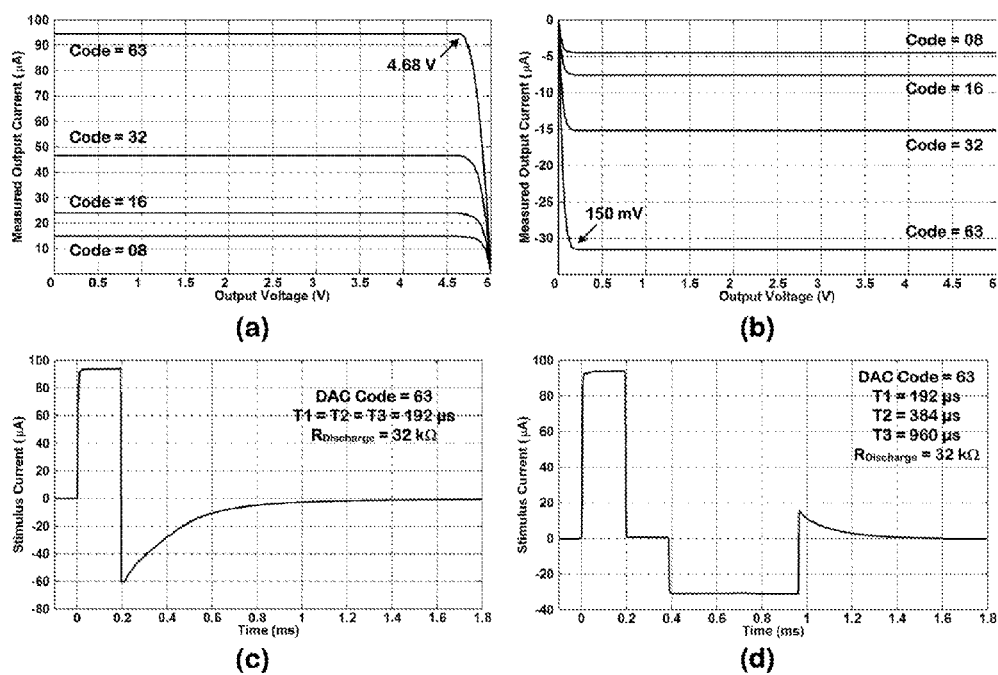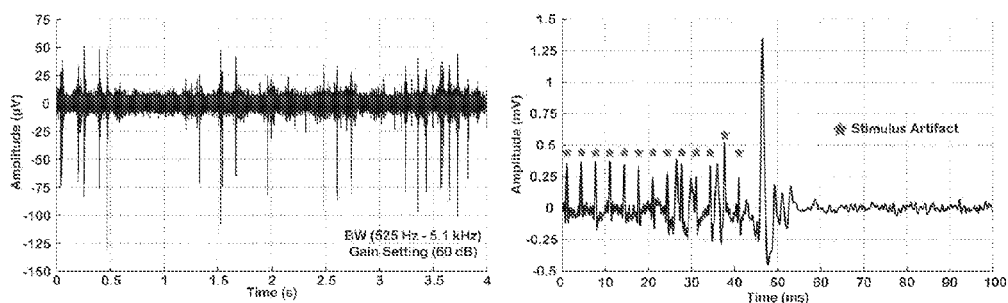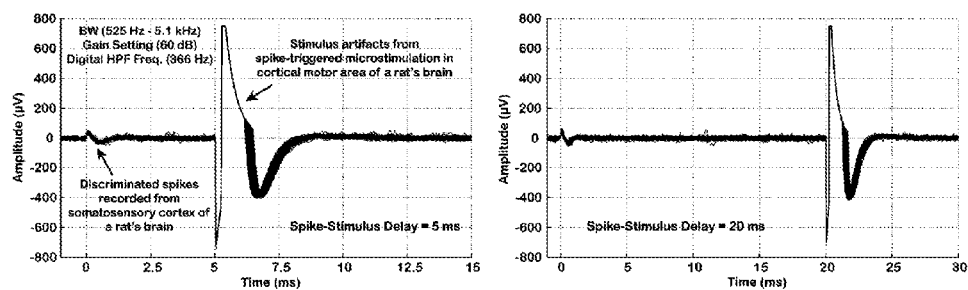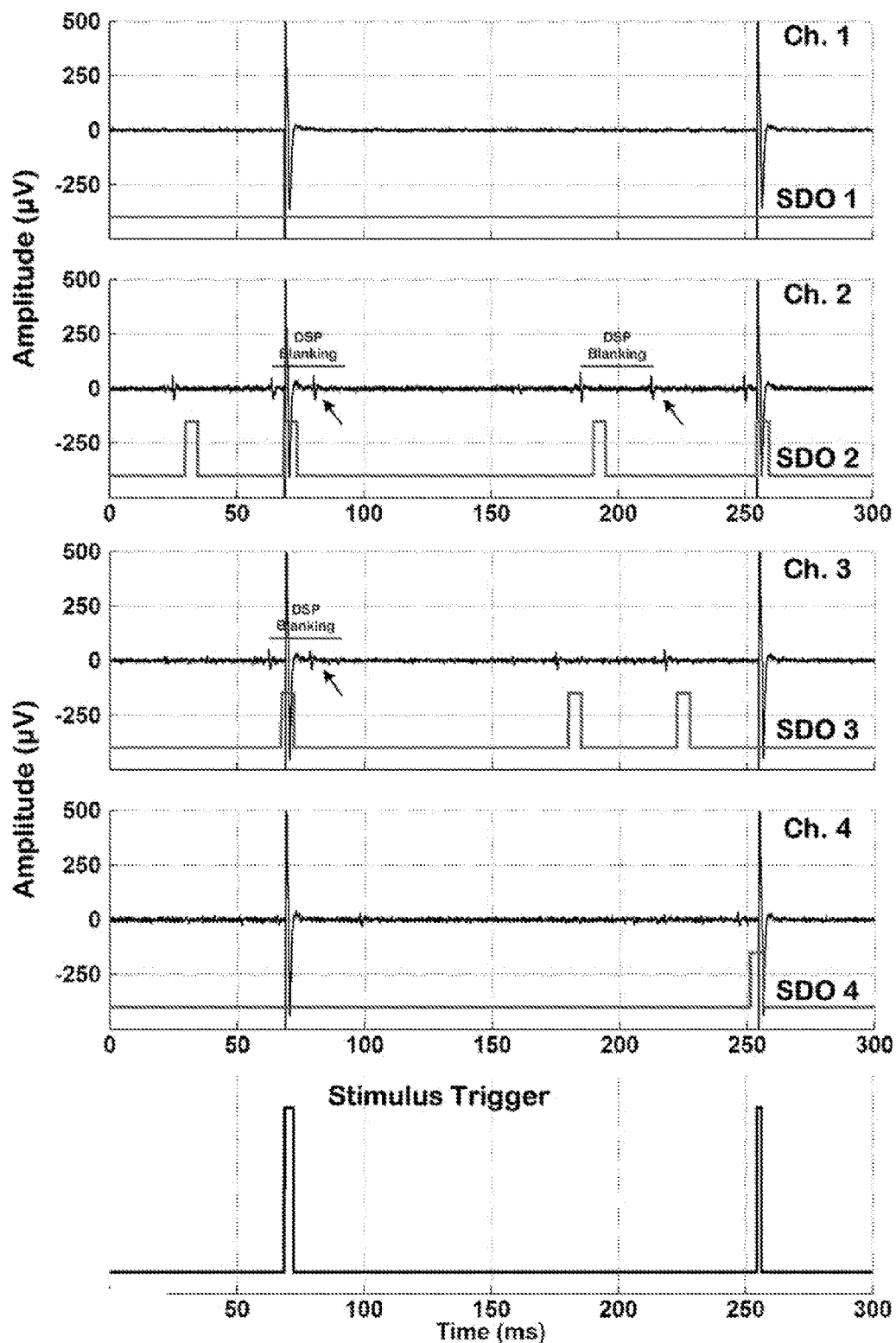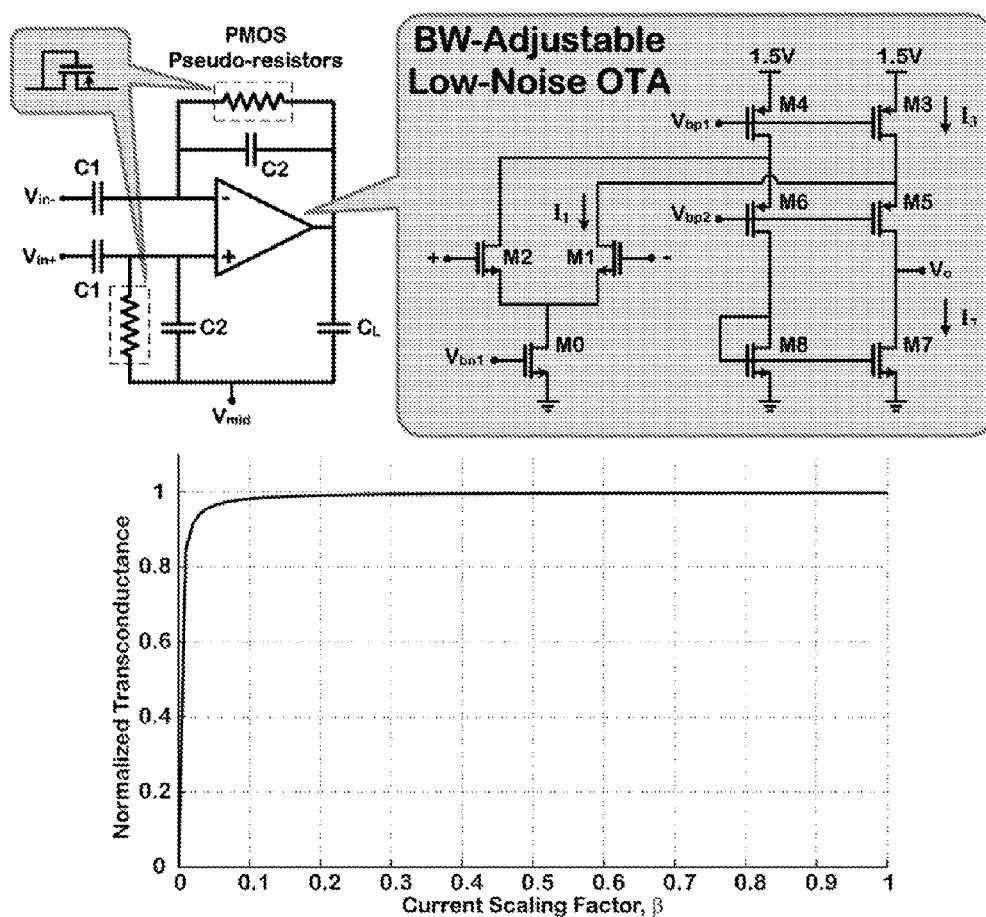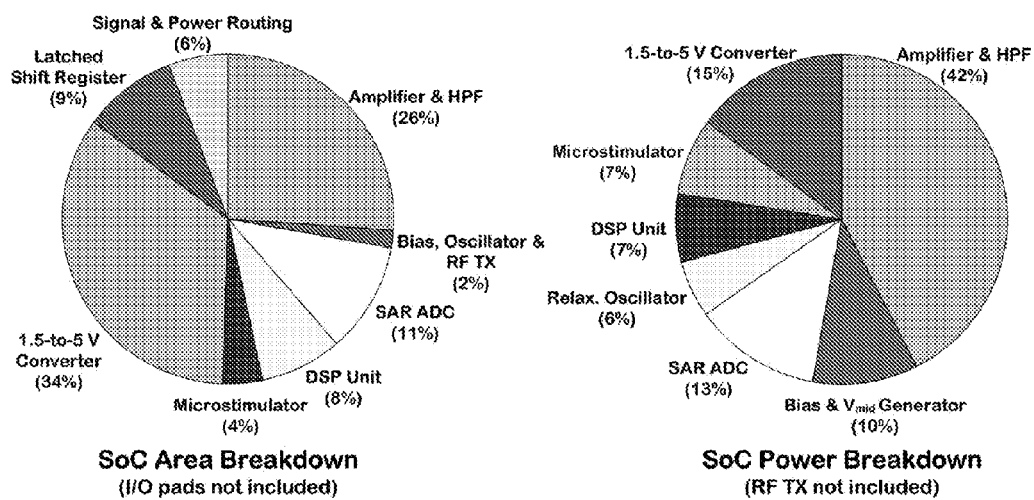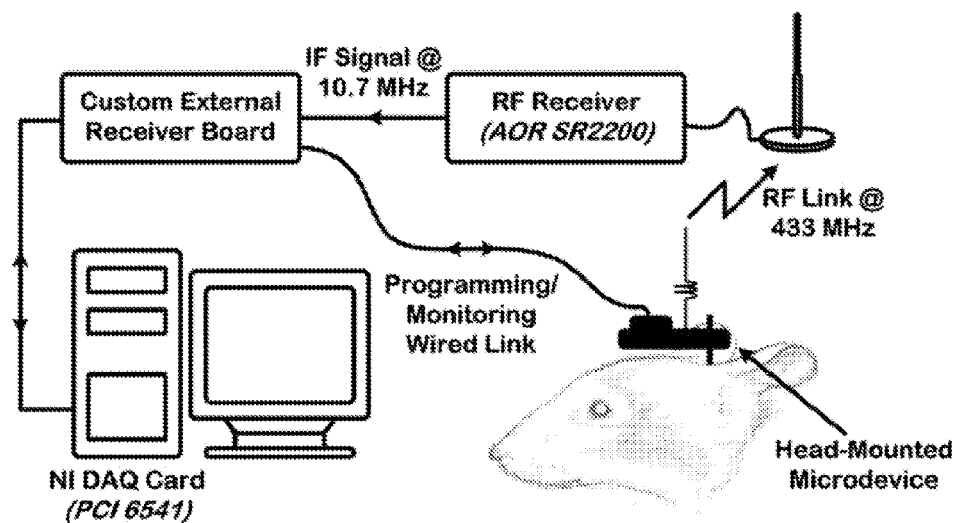

Figure 15
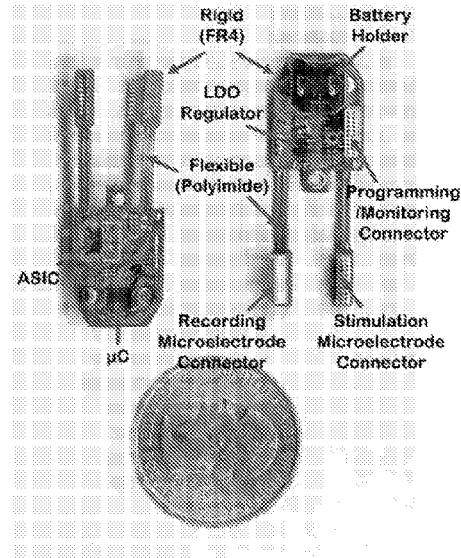
Figure 16

Figure 17

Figures 18A-18C

Figure 19

Figure 20
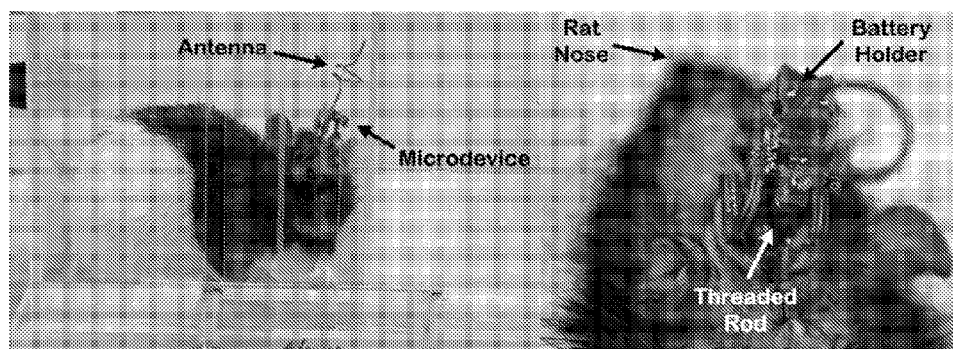
Figure 21
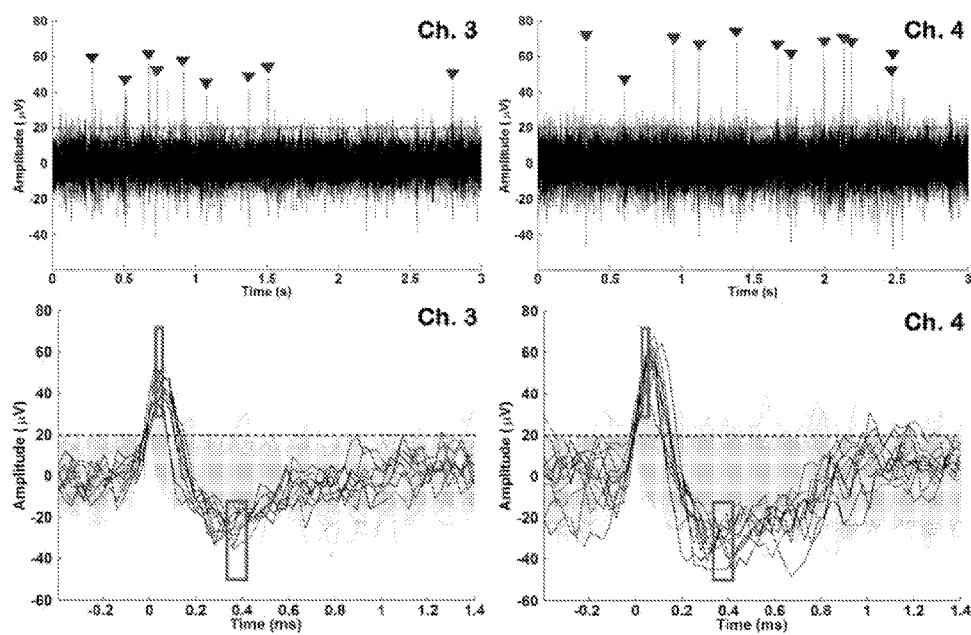
Figure 22
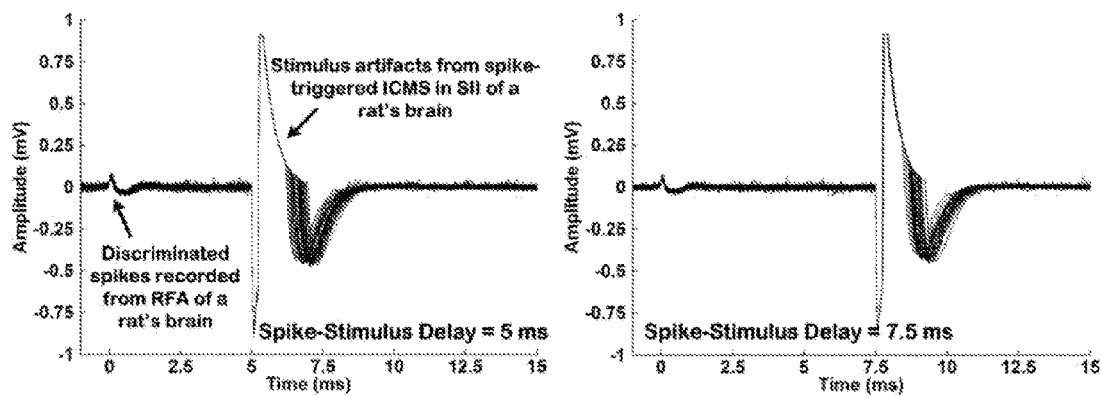
Figure 23
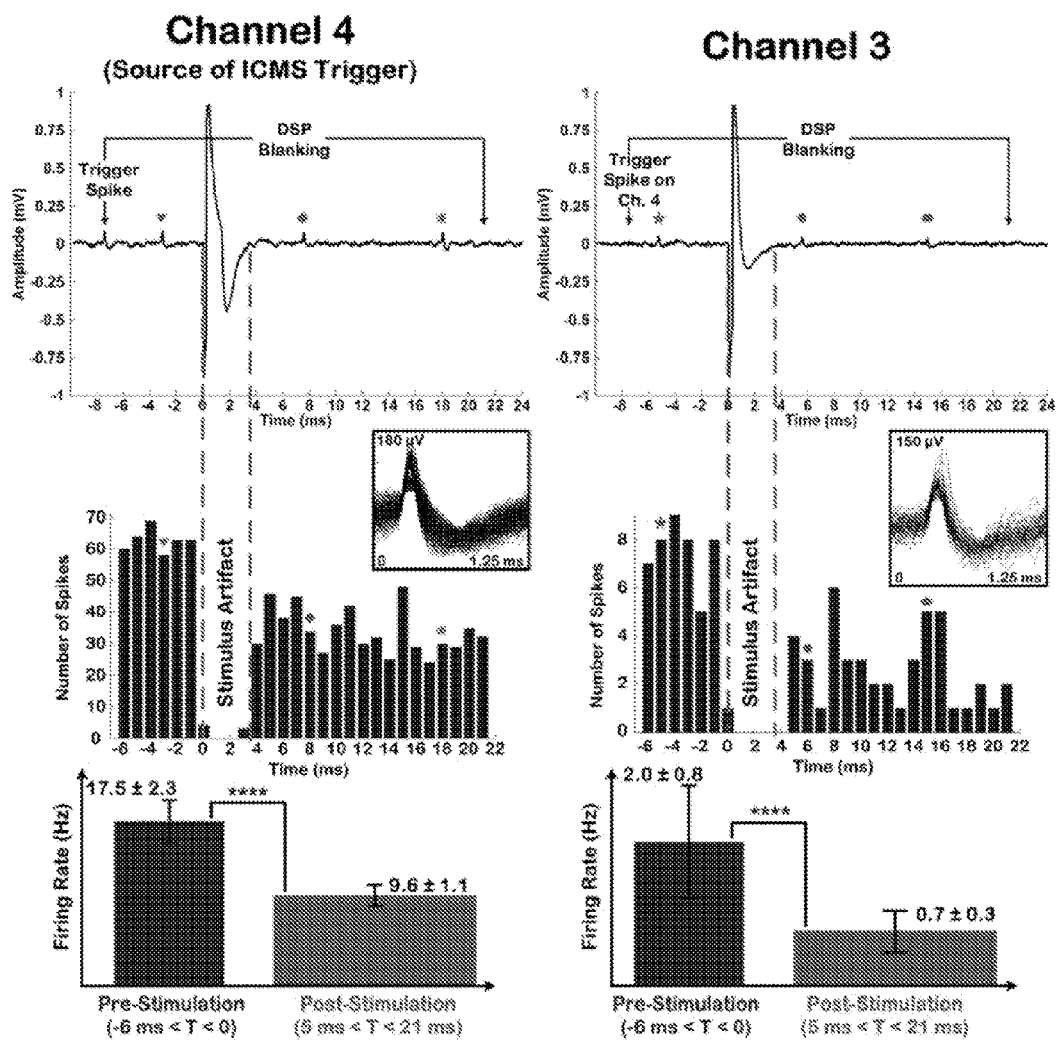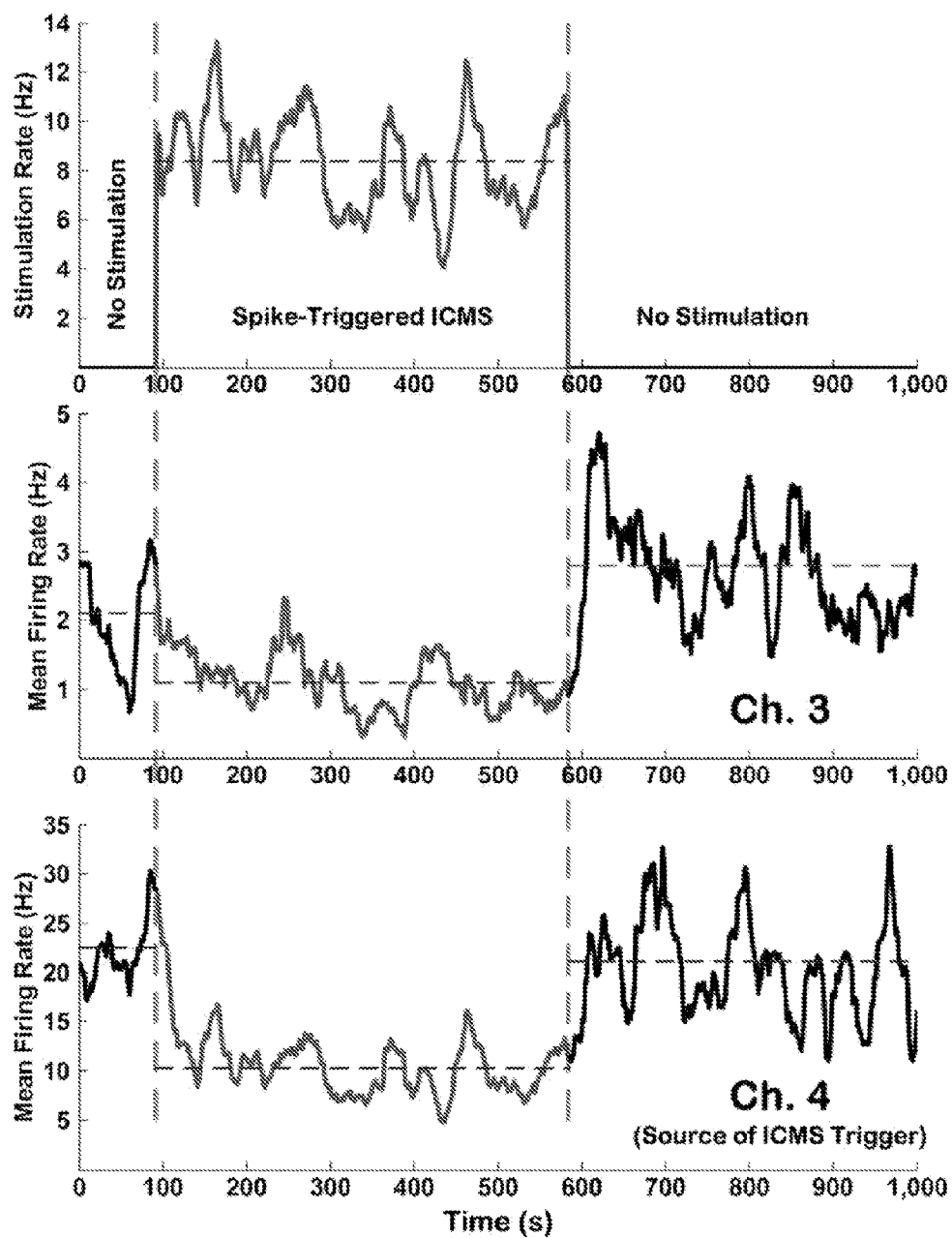
Figure 24

Figure 25A
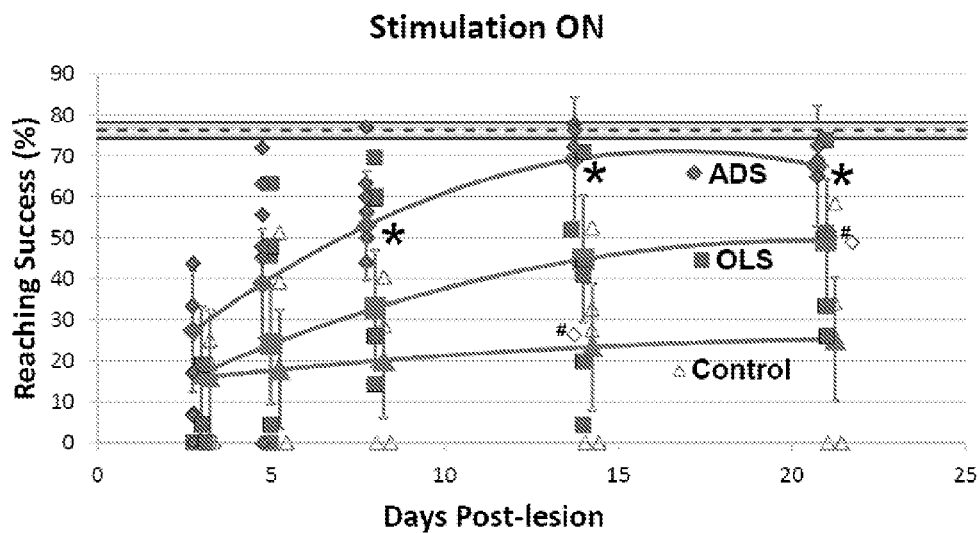
Figure 25B
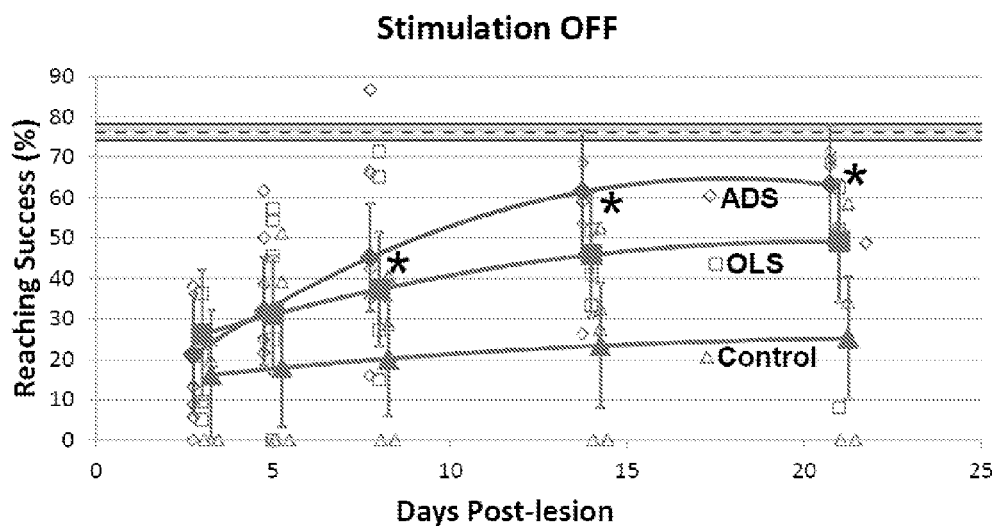
Figure 26
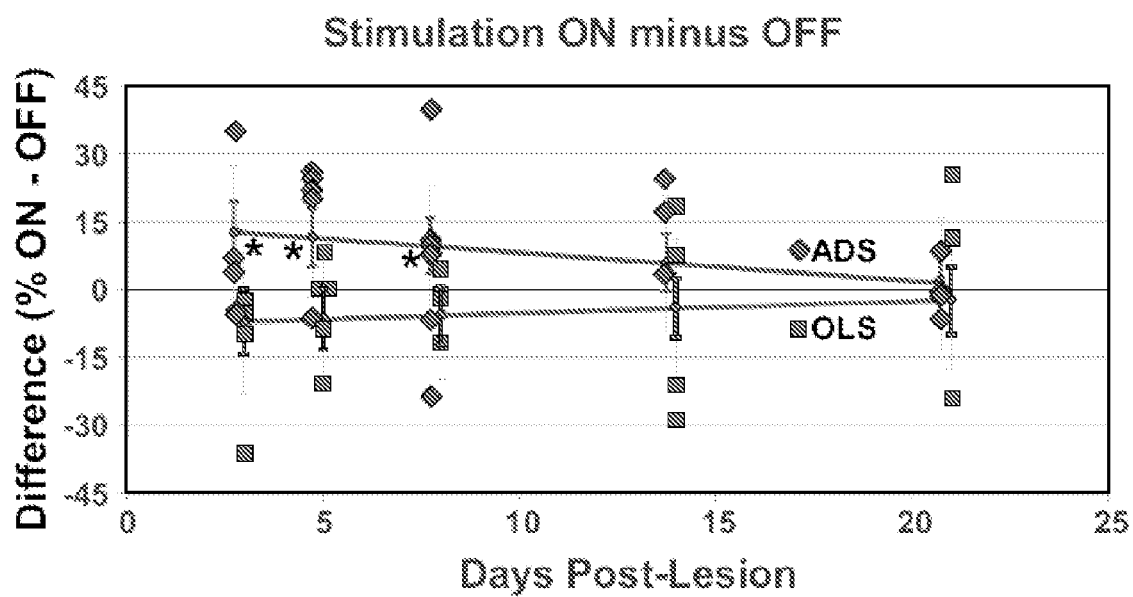
Stimulation ON minus OFF

METHODS AND ASSOCIATED NEURAL PROSTHETIC DEVICES FOR BRIDGING BRAIN AREAS TO IMPROVE FUNCTION

CROSS-REFERENCE TO RELATED APPLICATIONS

This application is a continuation of U.S. patent application Ser. No. 13/523,597, filed Jun. 14, 2012, which claims priority to U.S. Provisional Patent Application No. 61/543,593, filed Oct. 5, 2011, the entire contents of which are incorporated by reference herein.

STATEMENT OF GOVERNMENT INTEREST

This invention was made with government support under Grant Nos. W81XWH-08-1-0168, W81XWH-10-1-0741, and W81XWH-10-1-0742 awarded by the Department of Defense. The government has certain rights in the invention.

BACKGROUND

To date, brain-machine interfaces (BMIs) have sought to interface the brain with the external world using intrinsic neuronal signals as input commands for controlling external devices, or device-generated electrical signals to mimic sensory inputs to the nervous system. A new generation of neuroprostheses is now emerging that aims to combine neural recording, neural signal processing, and microstimulation functionalities in 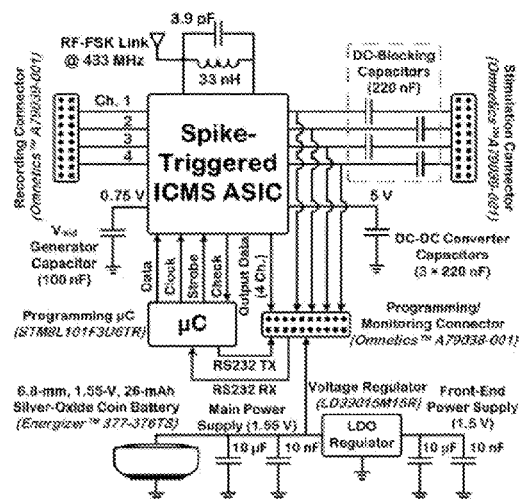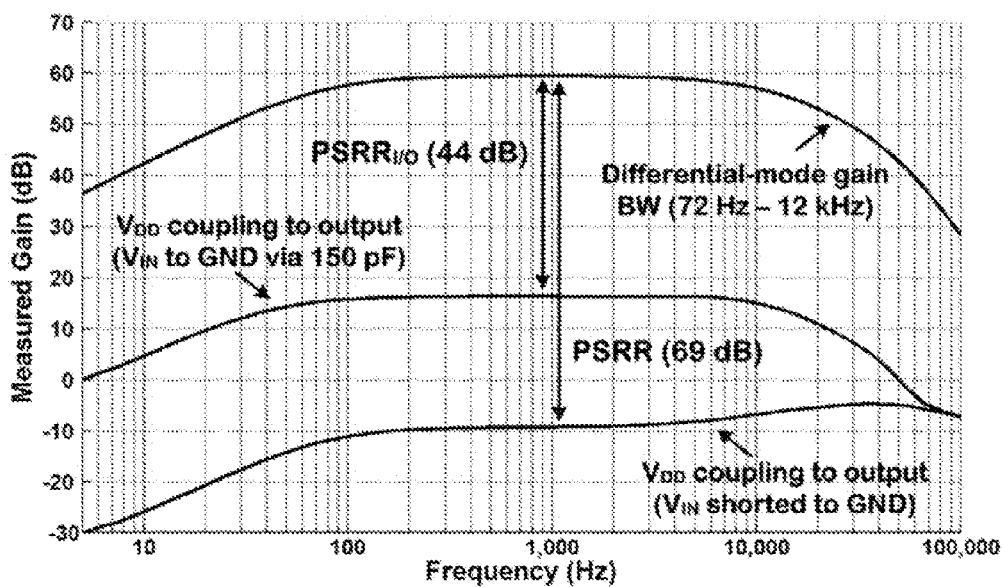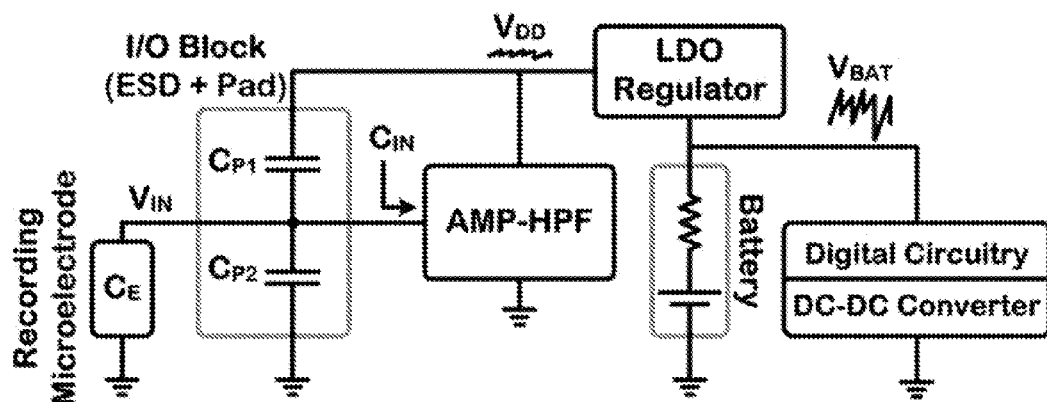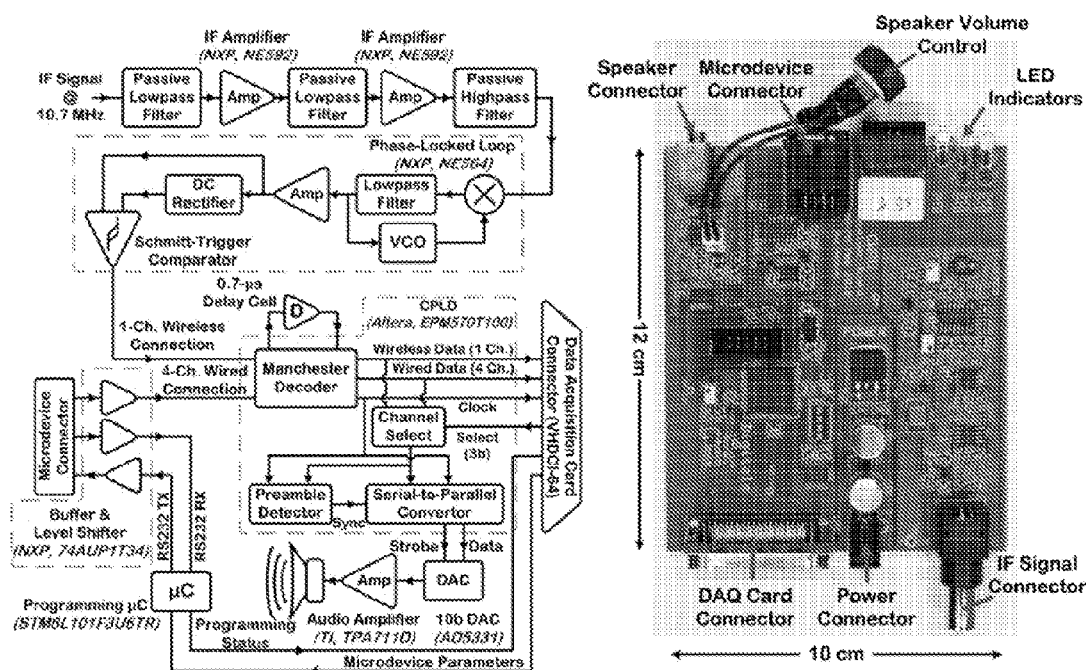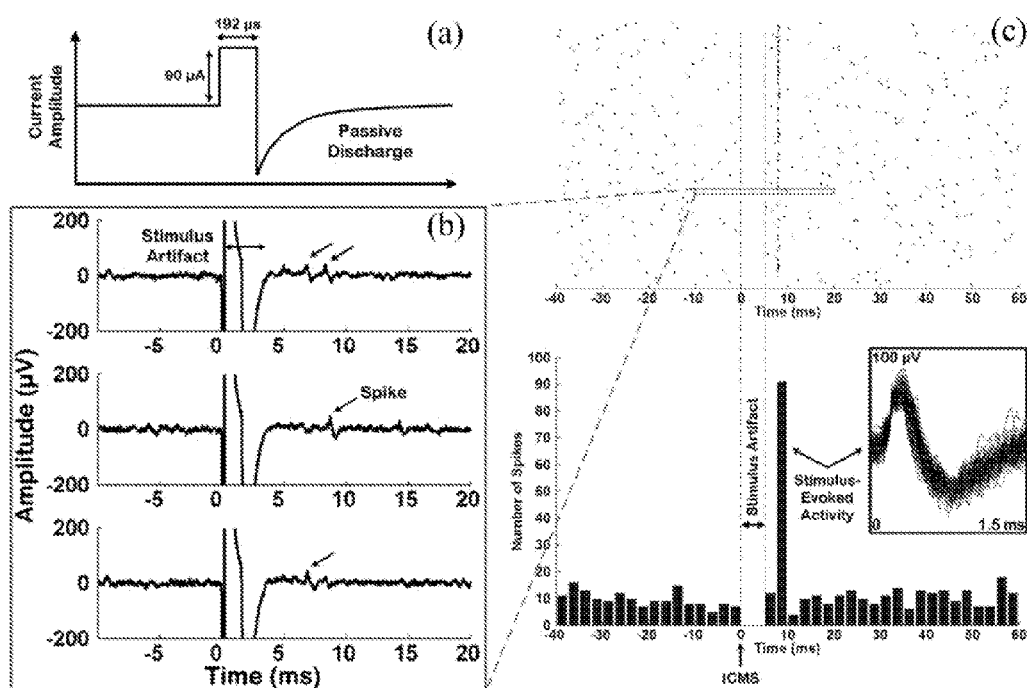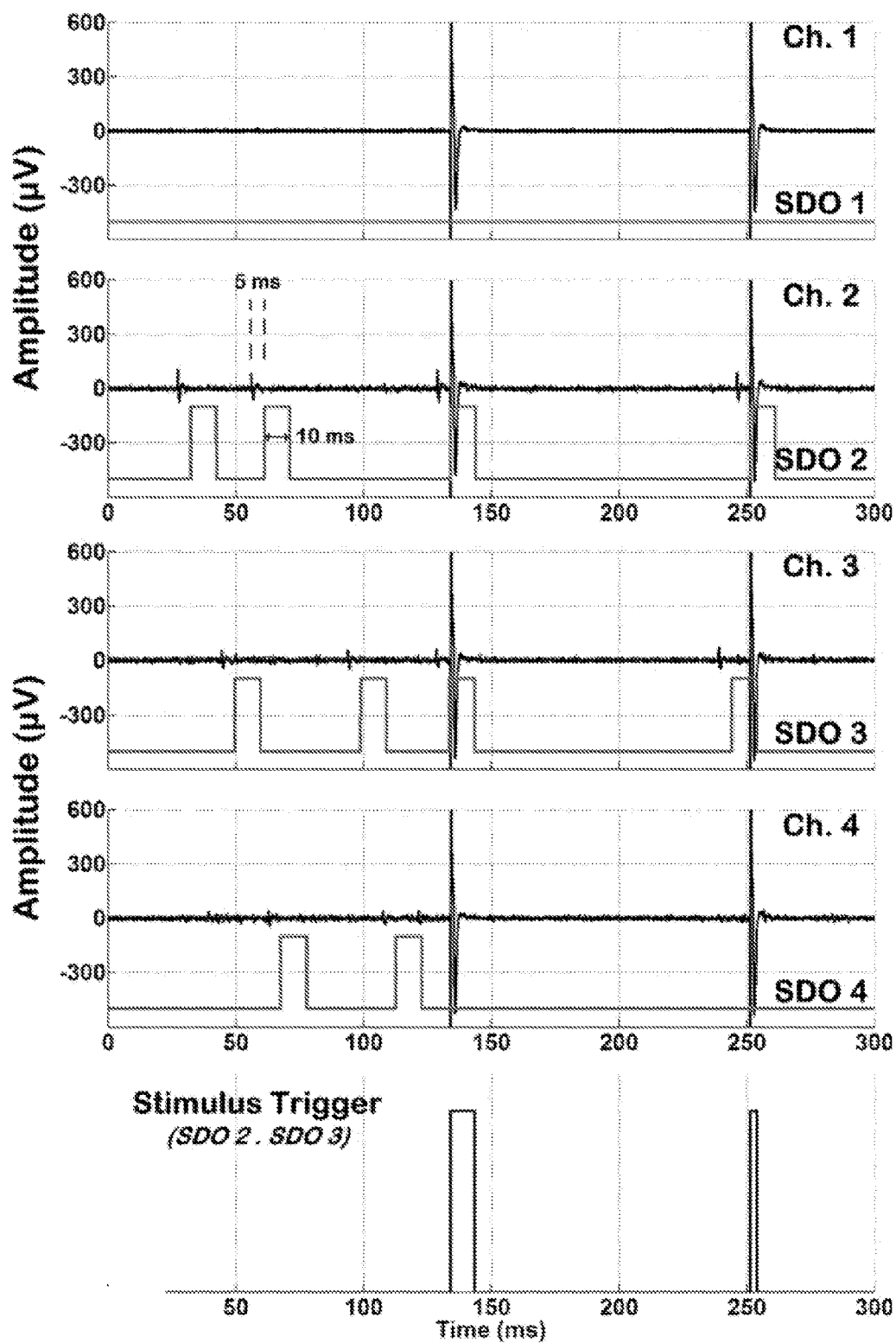a single device, creating an artificial connection in the nervous system by converting neural activity recorded from one cortical area to electrical stimuli delivered to another cortical area, spinal cord, or muscles in real time.

SUMMARY

The present disclosure generally relates to methods and associated neural prosthetic devices for bridging brain areas for the purpose of restoring or improving neurological function. More particularly, the present disclosure relates to, in one embodiment, multi-channel neural prosthetic devices and, in other embodiments, methods for utilizing a neural prosthetic device to function as a bridge between two neural sites between which there is substantially no effective communication.

The present disclosure provides neural prosthetic devices (i.e., microdevices) that successfully combine neural recording, signal processing, and microstimulation functionalities in a single device for closed-loop operation. Further, the present disclosure provides neural prosthetic devices that can operate autonomously and that convert extracellular neural signals recorded on one microelectrode to electrical stimuli delivered via another electrode in real time. In some embodiments, the methods of the present disclosure promote functional recovery after brain injury and are particularly suitable for reestablishing communication links between remote neural regions.

The devices and methods of the present disclosure may also be useful to provide activity-dependent neural stimulation to induce neuronal plasticity for functional reorganization in an intact nervous system, and have numerous applications such as restoring function after neuronal injury, providing refined sensory inputs in neuroprosthetic systems or supporting closed-loop therapeutic interventions for neuropathologies.

Accordingly, in one embodiment, the present disclosure provides a method comprising detecting a neural spike in a first neural site in a subject; and delivering a stimulus to a second neural site in the subject within a defined period of time after the detection of the neural spike, wherein there is substantially no effective communication between the first and second neural sites.

In another embodiment, the present disclosure provides a neural prosthetic device comprising an integrated circuit that comprises a recording front-end comprising a plurality of recording channels; a processor unit; and a stimulus delivering back-end comprising a plurality of stimulation channels.

In yet another embodiment, the present disclosure provides a method comprising providing a subject having a brain injury in which there is substantially no effective communication between a first neural site in the subject and a second neural site in the subject; detecting a neural spike in the first neural site; using a neural prosthetic device comprising a recording front-end, a processor unit, and a stimulus delivering back-end to deliver an electrical stimulus to the second neural site within a defined period of time after the detection of the neural spike; and allowing the neural prosthetic device to provide an effective communication bridge between the first and second neural sites.

The features and advantages of the present invention will be apparent to those skilled in the art. While numerous changes may be made by those skilled in the art, such changes are within the spirit of the invention.

DRAWINGS

Some specific example embodiments of the disclosure may be understood by referring, in part, to the following description and the accompanying drawings.

FIG. **1** depicts the proposed architecture and timing operation of a neural prosthesis for activity-dependent intracortical microstimulation (ICMS), suitable for use in the methods of the present disclosure. There are two identical 4-channel modules per chip powered by a single 1.5-V battery.

FIG. **2** is a circuit schematic of the analog recording front-end of one channel in a neural prosthesis suitable for use in the methods of the present disclosure.

FIG. **3** depicts the architecture of a digital signal processing (DSP) unit and operation of a time-amplitude window discriminator in a neural prosthesis suitable for use in the methods of the present disclosure. The flow chart for spike discrimination algorithm is also shown. Negative threshold level L_1 (not shown in bottom left) is used in the algorithm to discriminate waveforms with reverse polarity (i.e., negative-going initial portion), if necessary.

FIG. **4** is a circuit schematic of the microstimulating back-end of one channel in a neural prosthesis suitable for use in the methods of the present disclosure.

FIG. **5** is a die micrograph of a 3.3 mm×3.3 mm integrated circuit (IC) fabricated in 0.35-μm two-poly four-metal (2P/4M) complementary metal-oxide-semiconductor (CMOS) technology.

FIGS. **6A**-**6B** are graphs depicting (a) frequency response and (b) input noise voltage of an analog recording front-end of a neural prosthesis with different bandwidth settings. FIGS. **6C**-**6D** are graphs depicting the measured signal-to-noise and distortion ratio (SNDR) of the entire recording front-end at the successive approximation register analog-to-digital converter (SAR ADC) output versus (c) amplitude and (d) frequency of the input signal.

FIGS. **7**A-**7**B are graphs depicting measured microstimulator output current versus output voltage for four different digital-to-analog converter (DAC) input codes in (a) anodic and (b) cathodic phases. FIGS. **7**C-**7**D are graphs depicting measured (c) monophasic and (d) asymmetric biphasic stimulus current waveforms delivered by a neural prosthesis to saline via a microelectrode. Passive discharge is also performed in each case using an on-chip 32-kΩ resistor.

FIG. **8** is an in vivo demonstration of recording and stimulation functionalities of a neural prosthesis in an anesthetized rat. Left—Extracellular neural spikes recorded wirelessly from the somatosensory cortex of the brain. The data are shown after linear-phase offline filtering (500 Hz to 4 kHz) with spike amplitudes referred to the input. Right—Measured electromyogram (EMG) signal from the rat's neck muscle evoked by microstimulation of the cortical motor area with a train of 13 monophasic current pulses. The EMG signal was recorded by commercial electrophysiology equipment.

FIG. **9** depicts stimulation on one microelectrode in the cortical motor area of an anesthetized rat triggered by neural spikes discriminated on an adjacent microelectrode in the somatosensory cortex with spike-stimulus delays of 5 and 20 ms. Stimulus artifacts of <4 ms in duration were observed on the recording electrode. The data were recorded wirelessly with the amplitude levels referred to the input.

FIG. **10** depicts stimulation on one microelectrode in the cortical motor area of an anesthetized rat triggered by neural spikes discriminated on multiple recording sites of an adjacent microelectrode. The neural prosthesis was programmed to trigger ICMS when neural activity was discriminated on any two or more channels of the recording front-end. The timing parameters T_5, T_6 and T_7 in the DSP unit were set to 5, 10 and 28 ms, respectively. Arrows point to neural spikes on channels 2 and 3 that were not discriminated due to blanking of the DSP operation.

FIG. **11** is a simplified schematic of a low-noise amplifier (LNA) and its core operational transconductance amplifier (OTA) for noise analysis (top) and a plot of the normalized OTA transconductance G_m/g_{m1} versus a scaling factor β (bottom).

FIG. **12** is a chart depicting a break-down of the area and power consumption for an entire system-on-chip (SoC) of a neural prosthesis suitable for use in the methods of the present disclosure.

FIG. **13** is an illustration of the experimental setup from Example 2, depicting a head-mounted microdevice for spike-triggered ICMS in an ambulatory rat and peripheral devices for programming and monitoring.

FIG. **14** is a block diagram and a die micrograph of a 3.3 mm×3.3 mm application-specific integrated circuit (ASIC) for spike-triggered ICMS, suitable for use in the methods of the present disclosure.

FIG. **15** is a block diagram and a photograph of a fully assembled microdevice suitable for use in the methods of the present disclosure.

FIG. **16** depicts a mechanism for power supply rejection ratio (PSRR) degradation in an analog recording front-end when interfaced with a recording microelectrode. (Top) Block diagram. (Bottom) Measured PSRR with the input hardwired to ground as well as grounded via a 150-pF external capacitor.

FIG. **17** is a block diagram and a photograph of an external receiver board of a neural prosthesis suitable for use in the methods of the present disclosure.

FIGS. **18**A-**18**C depict neural response to ICMS. (a) Monophasic current pulse with passive discharge delivered

to the caudal forelimb area (CFA) of a rat's brain at 2 Hz. (b) Traces showing the neural response to ICMS. Arrows indicate spikes detected by the ASIC. (c) Raster plot and peristimulus histogram (2.5-ms bins) of the neural response to ICMS, showing an increase in neural activity after stimulation.

FIG. **19** is a graph showing the simultaneously recorded data on each channel of a multi-channel neural prosthesis at the output of the digital highpass filter (HPF) along with the corresponding spike discriminator output (SDO) and the resulting stimulus trigger signal during a 300-ms time window.

FIG. **20** depicts (Left) ambulatory rat instrumented with a microdevice inside a Plexiglas reaching chamber. (Right) Close-up view of the microdevice on top of the rat's head.

FIG. **21** depicts (Top) 3-s window of neural activity recorded on channels 3 and 4 of the microdevice in an ambulatory rat. (Bottom) Operation of the time-amplitude window discriminator. Spike waveforms in dark gray (and with blue markers in top plot) were accepted for stimulus triggering, whereas those in light gray were rejected by the spike discriminator.

FIG. **22** is a graph showing stimulation on the microelectrode implanted in the second somatosensory area (SII) triggered by neural spikes discriminated on the electrode implanted in the rostral forelimb area (RFA) with spike-stimulus delays of 5 and 7.5 ms. The data were recorded wirelessly with the amplitude levels referred to the input.

FIG. **23** depicts modulation of the neuronal firing rate due to ICMS triggered by neural spikes discriminated on one channel of a multi-channel neural prosthesis. (Top) 34-ms window of recorded data on channels 3 and 4, showing a stimulus artifact and neural spikes. (Middle) Peristimulus histogram of neural activity (1-ms bins) during DSP blanking period. (Bottom) Mean neuronal firing rate pre- and post-stimulation. Paired T-test showed the reduction in firing rate was statistically significant with p<0.0001. Insets depict the time-aligned and superimposed neural spikes in each histogram, except for those at t=0 (4 spikes on channel 4 and 1 spike on channel 3). The data were recorded via a wired link.

FIG. **24** depicts the modulation of neuronal firing rate due to ICMS triggered by neural spikes discriminated on one channel of a multi-channel neural prosthesis over a much longer time scale.

FIGS. **25**A-**25**B show a comparison of the success rate on the reaching task across groups after brain injury. Prior to brain injury (Day 0), all animals were required to reach a 70% baseline success rate on the reaching task. Dotted line indicates average pre-injury performance of all animals in the study. Shaded area indicates the 95% confidence interval. Following cortical impact, the microdevice was programmed to deliver appropriate stimulation. On behavioral testing days 3, 5, 8, 14 and 21, animals did 20 trials with the stimulation on (A) and 20 trials with the stimulation off (B). Regression lines are based on a linear mixed model. Individual data points are also superimposed on each graph. A) Comparison of reaching success between activity-dependent stimulation (ADS; red), randomized open-loop stimulation (OLS; green) and control (blue) animal groups when the stimulation was turned on during the trial (except in control group, which received no stimulation). B) Comparison between the three groups when the stimulation was turned off during the session. Reaching success was significantly better in the ADS group compared to the other groups on post-injury days 8, 14, and 21 in both the on and off states. In this and the following figure, error bars represent standard

error of the mean. *p<0.05 (difference between ADS group and both OLS and control groups). # Device not functioning.

FIG. 26 shows a comparison of the success rate on the reaching task within groups contrasting on and off stimulation states. On each of post-injury days 3, 5, 8, 14 and 21, reaching success with stimulation off was subtracted from reaching success with stimulation on. Activity-dependent stimulation (ADS) group is shown in red and open-loop stimulation (OLS) group is shown in green. On post-injury days 3, 5, 8 and 14, reaching success in the ADS group, but not the OLS group, was superior with stimulation on compared with stimulation off. *p<0.05 (difference between ADS and OLS groups).

The patent or application file contains at least one drawing executed in color. Copies of this patent or patent application publication with color drawing(s) will be provided by the Office upon request and payment of the necessary fee.

While the present disclosure is susceptible to various modifications and alternative forms, specific example embodiments have been shown in the figures and are herein described in more detail. It should be understood, however, that the description of specific example embodiments is not intended to limit the invention to the particular forms disclosed, but on the contrary, this disclosure is to cover all modifications and equivalents as illustrated, in part, by the appended claims.

DESCRIPTION

The present disclosure generally relates to methods and associated neural prosthetic devices (i.e., microdevices) for bridging brain areas for the purpose of restoring or improving neurological function. More particularly, the present disclosure relates to, in one embodiment, multi-channel neural prosthetic devices and, in other embodiments, methods for utilizing a neural prosthetic device to function as a bridge between two neural sites between which there is substantially no effective communication.

Methods

In one embodiment, a method of the present disclosure comprises detecting a neural spike in a first neural site in a subject and delivering a stimulus to a second neural site in the subject within a defined period of time after the detection of the neural spike, wherein there is substantially no effective communication between the first and second neural sites. In some embodiments, the detection of a neural spike and the corresponding delivery of a stimulus may be repeated continuously. As used herein, "effective communication" refers to temporally correlated activity between neurons that is necessary for normal behavioral function. Effective communication can either occur due to direct, physical connections between the neurons, or indirect connections via intermediate neural structures.

As would be recognized by one of ordinary skill in the art, the absence of effective communication between two or more neural sites may be generally known based on, for example, available literature, and experiments (e.g., tract-tracing, neurophysiology or neuroimaging (such as, e.g., diffusion-tensor imaging and resting-state connectivity)), or by utilizing any other method known to one of ordinary skill in the art for determining the absence of effective communication.

In one embodiment, the methods of the present disclosure may allow a neural prosthetic device to act as a communication bridge between two or more neural sites, including sites in different regions of the brain. In some embodiments, the neural sites may have substantially no effective commu-

nication. Suitable neural sites can be located in any region of the brain such as, for example, in a cortical region of the brain (e.g., in motor cortex, sensory cortex, frontal cortex, occipital cortex, temporal cortex or parietal cortex), corpus callosum, subcortical areas (e.g., thalamus, hypothalamus, limbic system, basal ganglia, amygdala, hippocampus), cerebellum, and olfactory bulb and/or tract. Further neural sites may be located in the spinal cord. Suitable sites outside of the brain and spinal cord include muscles. Accordingly, when used in subjects that have a cortical or subcortical communication disruption, which may be caused by an injury resulting from a stroke, a traumatic brain injury (TBI), a neurosurgical resection, a tumor, epilepsy, a spinal cord injury, etc., the methods of the present disclosure may provide the subject with functional recovery in the affected area. Such functional recovery may include, but is not limited to, improved speech, language comprehension, executive function, attention, memory, learning abilities, motor abilities and sensory abilities, as well as reduction in symptoms such as neglect, depression, spasticity, tremor, etc. In some embodiments, the methods of the present disclosure may serve to reduce symptoms of psychiatric disorders and autism spectrum disorders such as non-verbal communication skills, abnormal sensory perceptions, etc. In some embodiments, the methods of the present disclosure may serve to improve function in various types of disconnection syndromes, such as white matter dementia, conduction aphasia, disorders of consciousness, developmental dyslexia, tactile aphasia, etc. In some embodiments, the methods of the present disclosure may serve to improve function in certain types of disconnection syndromes beyond those involving a focal injury, such as Parkinson's disease. In some embodiments, the methods of the present disclosure may also serve as a guidance cue for regenerating or sprouting nerve fibers.

In some embodiments, the methods of the present disclosure also provide for a neural communication bridge in cortex or subcortical structures to alleviate functional disorders in idiopathic conditions, i.e., when specific dysfunctional communication cannot be identified. In some embodiments, the methods of the present disclosure also provide a neural communication bridge in cortex or subcortical structures to improve function or behavioral performance in otherwise healthy brains. Such methods may be implemented using a neural prosthetic device of the present disclosure.

Neural prosthetic devices suitable for use in the methods of the present disclosure will be further discussed in more detail below; however, such devices generally comprise an integrated circuit that comprises a recording front-end comprising one or more recording channels, a processor unit, and a stimulus delivering back-end comprising one or more stimulation channels.

In one embodiment, a neural spike in a first neural site may be recorded using a recording electrode that may be implanted in a subject at the first neural site and externally interfaced with one or more recording channels of a recording front-end of a neural prosthetic device. As would be recognized by one of ordinary skill in the art with the benefit of this disclosure, multi-site recording electrodes may be utilized in conjunction with a multi-channel neural prosthetic device so as to detect neural signals from a plurality of neural sites. Examples of suitable recording electrodes may include, but are not limited to, microelectrodes comprising silicon or tungsten with recording sites of iridium. Similarly, a recording electrode may be externally interfaced with a recording front-end of a neural prosthetic device in

any suitable manner, which may be temporary or permanent. In some embodiments, it may be desirable to interface a recording electrode with a recording front-end of a neural prosthetic device via a microconnector in a plug-and-play fashion so as to allow for disconnection in the event that the neural prosthetic device needs to be replaced or is no longer needed.

After a neural spike is recorded, it is transmitted to a processor unit comprising a spike discriminator that identifies whether the neural spike is acceptable as a stimulus trigger signal for a stimulus delivering back-end. In some embodiments, a spike discriminator identifies acceptable neural spikes by using a spike discrimination algorithm, which may utilize adjustable, user-set parameters. While one of ordinary skill in the art with the benefit of this disclosure would be able to determine suitable parameters, such exemplary parameters may consist of a threshold level and a time-amplitude window. Using this example, an acceptable neural spike would be one that crosses the threshold level and passes through the time-amplitude window. Furthermore, in certain embodiments, the multichannel recording capabilities add another level of rejection. Even if spike events are accepted based on the preceding criteria, they may represent random neuronal activity that is not closely related to the function of interest. By requiring the preceding criteria to be met on multiple recording channels, the user can further restrict triggering. This is accomplished by a decision-making algorithm in the DSP unit. User-set parameters can be adjusted to define the time window within which the multiple spike events occur.

In some embodiments, it may be advantageous to adjust user-set parameters to reduce or prevent false-triggering caused, at least in part, by stimulus artifacts. After an acceptable neural spike is detected and the stimulus delivering back-end stimulates a neural site, an artifact from the stimulation may falsely trigger a neural prosthetic device and initiate a second stimulation cycle. In an effort to avoid this, user-set parameters in the form of a threshold level and time-amplitude window in the processor unit may be adjusted to discriminate between stimulus artifacts and neural spikes. Additionally, blanking the processor unit operation after spike discrimination also prevents false-triggering.

If a neural spike, or a combination of neural spikes, is accepted as a stimulus trigger signal, then the stimulus delivering back-end will deliver a stimulus to a second neural site, or to a plurality of neural sites. Accordingly, a stimulus may be delivered to a second neural site using a stimulating electrode, which may be implanted in a subject at the second neural site and externally interfaced with one or more stimulation channels of a stimulus delivering back-end of a neural prosthetic device. Multi-site stimulation electrodes may be utilized in conjunction with a multi-channel neural prosthetic device so as to deliver a stimulus to a plurality of neural sites. As mentioned above with respect to recording electrodes, examples of suitable stimulation electrodes may include, but are not limited to, microelectrodes comprising silicon or tungsten with stimulation sites of iridium oxide. Similarly, a stimulation electrode may be externally interfaced with a stimulus delivering back-end of a neural prosthetic device in any suitable manner, which may be temporary or permanent. In some embodiments, it may be desirable to interface a stimulation electrode with a stimulus delivering back-end of a neural prosthetic device via a microconnector in a plug-and-play fashion so as to allow for disconnection in the event that the neural prosthetic device needs to be replaced or is no longer needed. A

recording electrode may likewise be interfaced with a recording front-end of a neural prosthetic device via a microconnector in a plug-and-play fashion. Furthermore, a flexible interconnect for interfacing an electrode with either the recording front end or the stimulus delivering back-end of a neural prosthetic device may be used in order to allow for some adjustability in microelectrode placement during implantation, simplifying the surgical procedure.

In some embodiments, the stimulation channel or channels of a stimulating back-end of a neural prosthetic device may comprise current-blocking capacitors to prevent any net dc current flow into the tissue contacted by a stimulation electrode, potentially arising from semiconductor failure or charge imbalance.

In some embodiments, it may be particularly advantageous to adjust the period of time between spike discrimination and stimulus onset. Such adjustability allows for patient-specific operation for optimized performance. For example, in some embodiments, the time period between which a neural spike is detected and a stimulus is subsequently delivered may be <1000 ms (e.g., <800 ms, <500 ms, <200 ms, <30 ms). In other embodiments, the time period may be reduced further, so as to achieve as little time lag as possible between a recorded spike and a stimulus (e.g., <20 ms, <10 ms, or <5 ms). In some embodiments, the particular period of time between spike discrimination and stimulus onset may be adjusted to replicate the normal timing relationships between the areas, which may depend on, among other things, distance, fiber size (e.g., larger fibers conduct at higher velocity), or whether interconnecting fibers are myelinated (e.g., faster conduction velocity in myelinated fibers).

In certain embodiments, the stimulus delivered may be an electric stimulus that may be monophasic or biphasic. In some embodiments, the stimulation may have an intensity of ≤ 10 mA (e.g., ≤ 5 mA, ≤ 1 mA, ≤ 500 μA, ≤ 300 μA, ≤ 100 μA) and duration of about 1 ms. Typically, current levels may range from 1 μA to 10 mA, depending largely upon electrode characteristics, and pulse duration may range from 50 μs to 1 ms (e.g., 200 μs). In certain embodiments, a train of pulses may be delivered per each trigger, ranging from 1 to 200 pulses.

In some embodiments, the method of spike recording and stimulus delivery may be repeated for a set amount of time such that a new communication link or links between two or more neural sites are established during performance of the method, after, or both. For example, the method may be performed for a period of 14 days, during which time a neural prosthetic device creates an artificial bridge between two or more neural sites, and after which time communication continues between the two or more neural sites, wherein there previously had existed substantially no effective communication between the two or more neural sites. The method may also be performed for a shorter or longer period of time (e.g., 8 days, 5 days, 30 days, or 60 days).

Neural Prosthetic Devices

In one embodiment, the methods of the present disclosure may be performed utilizing any neural prosthetic device capable of detecting a neural spike in a first neural site and delivering a stimulus to a second neural site within a defined period of time after detection. Examples of suitable neural prosthetic devices that may be utilized in the methods of the present disclosure include, but are not limited to, those devices disclosed in U.S. Patent Application Nos. 2009/0105786, 2007/0032738, 2006/0173259, 2005/0240242, 2005/0119703, 2006/0009814, 2007/0032834, 2007/0179584, 2007/01123932, and 2006/0200206.

In another embodiment, the present disclosure provides a neural prosthetic device, which may be utilized in the methods described above, comprising an integrated circuit that comprises a recording front-end comprising a plurality of recording channels; a processor unit; and a stimulus delivering back-end comprising a plurality of stimulation channels. The circuit is characterized as having a recording front-end that is operably connected to a stimulus delivering back-end such that a relevant recording of one or more neural spikes by the front-end can induce one or more relevant stimulations by the back-end. FIG. **1** depicts a specific exemplary embodiment of a neural prosthetic device of the present disclosure. Additionally, examples 1-3 below describe a specific embodiment of a neural prosthetic device comprising an integrated circuit that comprises a recording front-end comprising a plurality of recording channels, a processor unit, and a stimulus delivering back-end comprising a plurality of stimulation channels.

In some embodiments, a recording front-end of a neural prosthetic device of the present disclosure provides ac amplification, dc input stabilization, bandpass filtering and digitization to the recorded neural signals with fully programmable gain and bandwidth. Accordingly, in some embodiments, a recording front-end may comprise a low-noise amplifier (LNA), a highpass filter (HPF), a secondary amplifier and an analog-to-digital converter (ADC), specific examples of which are further discussed in the examples below. FIG. **2** depicts an exemplary circuit schematic of a recording front-end of a neural prosthetic device that includes a low-noise amplifier, a highpass filter, and a secondary amplifier, which also serves as an ADC driver. The ADC then converts the amplified neural signal into digitized form for further processing by the monolithic digital signal processing unit.

In some embodiments, a processing unit of a neural prosthetic device of the present disclosure may be a digital signal processing unit. In some embodiments, a digital signal processing unit suitable for use in the present disclosure may comprise a multiplexer, one or more filters (such as digital highpass filters), a spike discriminator, and decision circuitry used to generate a stimulus trigger signal. A multiplexer may allow for a multi-channel device to share the same processing unit. Upon determining that a neural spike is accepted as a stimulus trigger signal, a spike discriminator may send a stimulus trigger signal to a stimulus delivering back-end. FIG. **3** depicts an exemplary digital signal processing unit comprising a spike discriminator.

In some embodiments, a stimulus delivering back-end of a neural prosthetic device of the present disclosure may comprise, in addition to a plurality of stimulation channels, a stimulator timing control, a signal level shifter, and a digital-to-analog converter. As mentioned above, in some embodiments, the stimulus delivering back-end may have a user-adjustable time delay so as to deliver a stimulus at the desired period of time after neural spike discrimination. FIG. **4** depicts an exemplary circuit schematic of a stimulus delivering back-end of a neural prosthetic device.

In some embodiments, a neural prosthetic device of the present disclosure may also comprise a radio-frequency (RF) transmitter and a battery. In those embodiments where the neural prosthetic device comprises an RF transmitter, it may be used to transmit data to an external RF receiver. The data may consist of the neural signals and neural spikes on the multiple channels. Before transmitting the relevant data, a data serializer may be used to convert the recorded or processed data on each of the channels into a serialization

format that can be stored and transmitted. Additionally, a neural prosthetic device of the present disclosure may also be powered by a battery.

In certain embodiments, the present disclosure also provides a system for monitoring and programming a neural prosthetic device as described herein. The system may comprise a link for transmitting neural spikes and device data, an external receiver board that processes the transmitted data and receives and uses parameter data from a personal computer (PC) for programming a neural prosthetic device, a digital data acquisition (DAQ) card that establishes a connection between the external receiver board and a PC, a PC that stores the processed data and uses software to monitor and determine parameter data for programming a neuroprosthetic device.

To facilitate a better understanding of the present disclosure, the following examples of certain aspects of some embodiments are given. In no way should the following examples be read to limit, or define, the entire scope of the invention.

Example 1

A prototype chip was fabricated in 0.35-μm two-poly four-metal (2P/4M) CMOS as shown in FIG. **5**, measuring 3.3 mm×3.3 mm including the bonding pads. This example discusses the measurement results from benchtop characterization and acute biological experiments with rats.

Benchtop Characterization

The top plots in FIG. **6** depict the measured frequency response and input-referred noise voltage spectrum of the analog recording front-end for three different bandwidth settings and with the midband ac gain nominally set to 60 dB. The low cutoff frequency could be programmed from 1.1 to 525 Hz, whereas the high cutoff frequency could be adjusted in the range of 5.1 to 12 kHz. The midband ac gain was measured to be 51.9, 57.4, 59.9 and 65.6 dB when the G_m-C HPF was bypassed. The gain dropped by ~0.3 dB when the HPF was included in the signal path. With the bandwidth set to 1.1 Hz to 12 kHz, the thermal noise level was measured to be 21 nV/rtHz at 1 kHz. This level increased as the bandwidth decreased, because the LNA input transistors carried less current, increasing their thermal noise contribution. With the same bandwidth setting, the total input noise voltage was measured to be 3.12 μV_{rms} by integrating the noise spectrum from 0.5 Hz to 50 kHz, indicating an increase of only 8.2% due to flicker noise. This led to a noise efficiency factor (NEF) of 2.68 for the LNA. The flicker noise corner frequency was measured to be <90 Hz for all bandwidth settings, indicating that the G_m-C HPF could largely reduce the flicker noise contribution.

A sinusoidal signal with varying amplitude and frequency was then applied to the LNA input and the signal-to-noise and distortion ratio (SNDR) was measured at the ADC output. FIG. **6**(c) shows the measured SNDR at 1 kHz versus input amplitude for the four available gain settings. Lower gain values provided higher input dynamic range, whereas higher gain values provided better signal resolution. FIG. **6**(d) depicts the measured SNDR versus input frequency. In the frequency range of 100 Hz to 10 kHz for extracellular neural spikes, the recording front-end provided >41.8 dB of accuracy.

The top plots in FIG. **7** depict the measured microstimulator output current versus its output voltage in the anodic and cathodic phases for four different DAC input codes. The stimulator output voltage could reach at least 4.68 V (going toward 5 V) and 150 mV (going toward 0 V) with a 5-V

supply. To further examine the microstimulator functionality, it was interfaced with a silicon-substrate micromachined electrode with stimulus sites of iridium oxide (IrO). FIGS. 7(c) and (d) depict the measured monophasic and asymmetric biphasic stimulus current waveforms delivered by the chip to saline via the microelectrode. The power consumption per channel was measured to be 3.5 µW from 5 V, when the microstimulator generated the biphasic waveform in FIG. 7(d) at a rate of 33 Hz. Table 1 summarizes the measured performance of major circuitry.

TABLE 1

Summary of Measured Performance

Recording Front-End	
AC Gain @ 1 kHz	51.9, 57.4, 59.9, 65.6 dB
Low Cutoff Freq.	1.1~525 Hz
High Cutoff Freq.	5.1~12 kHz
Total RMS Input	3.12 µV (BW of 12 kHz)
Noise Voltage	3.42 µV (BW of 5.1 kHz)
NEF	2.68 (BW of 12 kHz)
	2.9 (BW of 5.1 kHz)
CMRR @ kHz	>56 dB
PSRR @ 1 kHz	>65 dB
Crosstalk	<−72 dB
Max. Sampling Freq.	63 kS/s
INL/DNL	<±0.8 LSB
ENOB	9.2 b (f_{in} = 1 kHz, f_s = 35.7 kS/s)
	9.1 b (f_{in} = 1 kHz, f_s = 63 kS/s)
Power Consumption*	
Amp-HPF	26.9 µW (BW of 12 kHz)
SAR ADC	19.9 µW (BW of 5.1 kHz)
	5.9 µW (f_{CLK} = 1 MHz)
Digital Signal Processing Unit	
HPF Cutoff Freq.	366/756 Hz (f_{CLK} = 1 MHz)
Power Consumption	12.4 µW (f_{CLK} = 1 MHz)
Relaxation Oscillator	
Output Frequency	420 kHz~2.5 MHz
Supply Sensitivity	−60 kHz/V
Power Consumption	20.8 µW (f_{CLK} = 1 MHz)

Microstimulating Back-End	Anodic	Cathodic
Stimulus Waveform	Asymmetric Biphasic & Monophasic w/Passive Discharge	
Output Current	0~94.5 µA	0~31.5 µA
Current Pulsewidth		
Monophasic	0~1.008 ms	N/A
Biphasic	0~240 µs	0~720 µs
Output Impedance	~400 MΩ	~440 MΩ
DAC Resolution	6 b	
DAC Linearity	<±1.6 LSB	
Supply Sensitivity	−70.4 nA/V	−10.4 nA/V
Voltage Compliance		
Monophasic	4.68 (of 5 V)	N/A
Biphasic**	3.18 (of 3.5 V)	1.35 (of 1.5 V)
Current Efficiency	95.6% (I_{out} = 94.5 µA)	N/A

1.5-to-5 V Converter	
DC Output Voltage	4.86~5.35 V
Output Ripple	40 mV_{pp}
Max. Load Current	88 µA (V_{out} = 5.05 V)
Power Efficiency	31% (V_{out} = 5.05 V)
RF Transmitter	
Comm. Scheme	FSK @ 433 MHz
Received Power @	−55 dBm (18-cm monopole

TABLE 1-continued

Summary of Measured Performance

1 m	TX and RX Antennae)
Power Consumption	200 µW

Total Power for Two Modules w/o RF TX (Stimulation Rate = 33 Hz, Recording BW = 525 Hz~5.1 kHz) = 375 µW
*Per channel

In Vivo Characterization

In the first biological experiment, a silicon microelectrode with recording sites of iridium was implanted in the somatosensory cortex of a rat's brain and externally interfaced with a single channel of the recording front-end on the chip. The left plot in FIG. 8 shows a 4-s snapshot of the extracellular neural spikes recorded wirelessly at the output of the ADC. In another test, a tungsten electrode with impedance value in the range of 50 to 100 kΩ was placed in the cortical motor area and externally interfaced with a single channel of the microstimulating back-end on the chip to stimulate the brain with a train of 13 monophasic current pulses (90 µA, 192 µs, 300 Hz). The right plot in FIG. 8 depicts the evoked electromyogram (EMG) signal recorded from the rat's neck muscle. The largest EMG spike appeared in <50 ms from the stimulation onset. The chip was then interfaced with the two implanted electrodes to demonstrate activity-dependent ICMS and programmed with the time-amplitude window discriminator parameters determined empirically prior to the experiment. In the first test, the recording and stimulation electrodes were each connected to a single channel of the front- and back-end on the chip, respectively. As the chip operated fully autonomously from a 1.5-V battery, it successfully delivered electrical stimuli to the cortical motor area triggered by neural spikes discriminated on the adjacent electrode in the somatosensory cortex, producing an artificial connection between the two brain regions. FIG. 9 shows the superimposed spike waveforms and corresponding stimulus artifacts from single-pulse stimulation (90 µA, 192 µs) with spike-stimulus delays of 5 and 20 ms. The stimulus artifact rejection mechanism in the recording front-end was de-activated in this test. Hence, artifacts of <4 ms in duration were observed on the recording electrode.

Finally, while the stimulation electrode remained connected to a single channel of the back-end, the multisite recording electrode was connected to all four channels of the front-end in one module. The decision-making circuitry was programmed to trigger ICMS whenever neural activity would be present on any two or more data channels. FIG. 10 shows a 300-ms snapshot of the recorded data of each channel at the output of the digital HPF along with the corresponding spike discriminator output (SDO) and the resulting stimulus trigger signal. Two large stimulus artifacts were distinguishable on each channel. The first stimulation was triggered by neural activity on channels 2 and 3, whereas the second was due to neural activity on channels 2 and 4. Some recorded spikes (marked by black arrows) were not discriminated by the DSP unit due to blanking of its operation after discriminating the spikes that immediately preceded them. This can be alleviated by reducing the time duration of DSP blanking.

As seen in FIGS. 9 and 10, stimulus artifacts are used in this work to show that stimulation is occurring in vivo. However, to address the concern of artifacts false-triggering the microstimulator, a time-amplitude window discriminator is used (as opposed to simple spike thresholding) to discriminate between neural spikes and stimulus artifacts by

proper adjustment of time-amplitude window parameters. Blanking the DSP operation after spike discrimination also prevents false-triggering the stimulator by the incoming stimulus artifact. Another concern related to stimulus artifacts is that any spike activity that occurs within the duration of the artifact cannot be detected by the system for triggering purposes. This is less of a concern for activity-dependent microstimulation, since we do not foresee a need to use every single spike in the system to entrain a neuronal population to another group of neurons. Nonetheless, we are developing an integrated signal-processing solution for real-time stimulus artifact rejection, which affords to retain signal information during each stimulation cycle. Such capability may be added to the DSP unit.

LNA Noise Analysis

This section presents a noise analysis for the selected LNA topology and obtains a minimum NEF for a practical design given our technology parameters and supply voltage. FIG. 11 shows a simplified schematic of the LNA and its core operational transconductance amplifier (OTA) for this analysis. We also model the transistor thermal noise current as

$$\overline{i_n^2} = 4KT \times \gamma \times g_m \tag{1}$$

where K is the Boltzmann's constant, T is the absolute temperature, g_m is the transistor transconductance, and γ is $\frac{2}{3}$ for a transistor operating in strong inversion (above-threshold) and $1/(2\kappa)$ for a transistor operating in weak inversion (subthreshold) in which κ is the subthreshold gate coupling coefficient with a typical value of 0.7. The transistor transconductance can be estimated as

$$g_m \approx \frac{\kappa \times I_D}{V_{th}} \quad \text{Weak inversion } (subthreshold) \tag{2}$$

$$g_m \approx \frac{2 \times I_D}{V_{OD}} \quad \text{Strong inversion (above-threshold)}$$

where V_{th} is the thermal voltage, I_D is the transistor drain current, and V_{OD} is the transistor overdrive voltage. Assuming that the overall transconductance of the OTA, G_m, is nearly equal to that of transistor M_1, the input-referred noise voltage of the OTA can be estimated as

$$\overline{V_{n,OTA}^2} = \frac{1}{g_{m1}^2} \left(\frac{4KT}{\kappa} \times g_{m1} + \frac{16KT}{3} \times g_{m3} + \frac{16KT}{3} \times g_{m7} \right). \tag{3}$$

To minimize the OTA input noise voltage, $M_{1,2}$ operate in subthreshold to maximize g_{m1} for a given current level, whereas $M_{3,4,7,8}$ operate in strong inversion to reduce their transconductances. Moreover, the drain current of $M_{1,2}$ is selected to be much larger than that of $M_{7,8}$ in the folded branch. This current scaling scheme helps improve the OTA noise performance by further increasing g_{m1} and reducing $g_{m7,8}$. Therefore, neglecting the noise contribution by $M_{7,8}$, (3) can be simplified as

$$\overline{V_{n,OTA}^2} = \frac{1}{g_{m1}} \times \frac{4KT}{\kappa} \left(1 + \frac{8}{3} \times \frac{V_{th}}{V_{OD3}} \times (\beta + 1) \right) \tag{4}$$

where $\beta = I_7/I_1$ is the current scaling factor between the input differential pair and the folded branch. Equation (4) suggests that V_{OD3} should be increased to reduce the OTA input

noise. However, increasing V_{OD3} means the drain-source voltage of $M_{3,4}$ should be increased too, limiting the OTA output voltage swing. For a peak-to-peak voltage swing (V_{Swing}) of 0.5 V at the OTA output, an upper limit of 0.5 V can be found for V_{OD3} given a supply voltage of 1.5 V. It should be noted that V_{Swing} of 0.5 V allows the LNA to handle input signals as large as ~±6 mV, in case local field potentials (LFPs) or other low-frequency artifacts would also be present at the input. In this work, $M_{3,4}$ are sized for V_{OD3} of 0.35 V instead to ensure that they do not enter the triode region in the presence of process parameter variation.

According to (4), the OTA input noise voltage also depends on β, indicating that the current scaling factor should be selected judiciously. To that end, we next investigate the effect of β on the overall OTA transconductance, G_m. In a similar way, the analysis of the proposed circuit reveals the G_m to be

$$G_m \approx \frac{g_{m5}}{g_{ds1} + g_{ds3} + g_{m5}} \times g_{m1} \tag{5}$$

where g_{ds} is the transistor drain-source conductance. Since the channel length of $M_{3,4}$ is selected to be much longer than that of $M_{1,2}$, g_{ds3} is much smaller than g_{ds1}, which yields

$$\frac{G_m}{g_{m1}} \approx \frac{1}{1 + \dfrac{V_{th}}{\kappa \times V_{A1} \times \beta}} \tag{6}$$

where V_{A1} is the early voltage for M_1 (i.e., $1/\lambda_1$) and M_5 is sized to operate in subthreshold. This equation is also plotted in FIG. 11 with a value of 20 V for V_{A1}. According to (4), reducing β helps reduce the OTA input noise voltage, but β cannot be reduced arbitrarily to ensure that G_m is not degraded considerably (i.e., $\beta \geq 0.05$ from FIG. 11).

Another important consideration in selecting β is the sensitivity of bias currents to transistor mismatches in the OTA and associated biasing circuitry. Assume that ΔI_1, ΔI_3 and ΔI_7 are bias current deviations from their corresponding nominal values due to transistor mismatches. If ΔI_1 and ΔI_3 are assumed to be uncorrelated, it can be shown that

$$\frac{\Delta I_7}{I_7} = \sqrt{\frac{\Delta I_1^2 + \Delta I_3^2}{I_7^2}} \tag{7}$$

$$= \frac{1}{\beta} \times \sqrt{\left(\frac{\Delta I_1}{I_1}\right)^2 + (\beta + 1)^2 \times \left(\frac{\Delta I_3}{I_3}\right)^2}.$$

For example, for a β value of 0.05, a 2% variation in I_1 and I_3 causes a 58% variation in I_7, which might adversely affect the OTA operation and degrade its transconductance. In this example, the minimum value of β (when LNA bandwidth is maximum) is selected to be 0.091 for which G_m is 98% of g_{m1}, and 2% variation in I_1 and I_3 causes only 32.5% variation in I_7. Table 2 tabulates the dimension, current level, and operating condition of each transistor pair in the OTA for optimum noise performance with the maximum bandwidth setting.

TABLE 2

	Dimension, Current Level, and Operating Condition of OTA Transistors				
Transistor	Dimension (µm)	Current Level (µA)	Simulated g_m (µS)	Inversion Coefficient*	Operating Condition
$M_{1,2}$	800/2	2.75	76	0.021	subthreshold
$M_{3,4}$	20/20	3.00	16	26.8	above-threshold
$M_{5,6}$	80/1.3	0.25	6.9	0.036	subthreshold
$M_{7,8}$	4/40	0.25	2.5	7.6	above-threshold

*$\mu_n C_{ox}$ = 170 µA/V^2, $\mu_p C_{ox}$ = 58 µA/V^2

To compute the NEF, we should note that the input-referred noise voltage of the LNA is almost equal to that of the OTA given that the parasitic gate capacitance at the input terminals of the OTA is typically much smaller than $C_{1,2}$. The NEF can be calculated according to

$$NEF = V_{ni,rms} \times \sqrt{\frac{2 \times I_{total}}{\pi \times V_{th} \times 4KT \times BW}} \qquad (8)$$

where $V_{ni,rms}$ is the rms input noise voltage of the LNA, I_{total} is the total supply current, and BW is the 3-dB bandwidth of the amplifier. Finally, assuming that the LNA has a single dominant pole in its frequency response and noting that $I_{total}=2 \times I_3$, combining (4) and (8) yields

$$NEF = \sqrt{\frac{2 \times (\beta + 1)}{\kappa^2} \times \left(1 + \frac{8}{3} \times \frac{V_{th}}{V_{OD3}} \times (\beta + 1)\right)} \qquad (9)$$

which results in an NEF of 2.33 for β of 0.091 and V_{OD3} of 0.35 V. Hence, the NEF of 2.68 derived from measured performance of the LNA (when set for maximum bandwidth) is in good agreement with this analysis. This argument also shows that reducing the supply voltage can adversely impact the OTA noise performance for the same output voltage swing, making it challenging to reduce the power supply (or V_{DD}) below 1.5 V in this architecture.

Other embodiments of a neural prosthetic device might require 16, 32 or even higher number of recording and stimulating channels, resulting in higher power consumption and larger silicon area. FIG. 12 shows a breakdown of the area and power consumption for the entire SoC, including both modules. The core area of the SoC excluding I/O pads is 2.6×2.6 mm², of which 34% is occupied by the 1.5-to-5-V converter. In this work, the converter can provide a maximum dc load current of ~88 µA for an output voltage of 5.05 V, which allows an average stimulus rate of >500 Hz for simultaneous stimulation on all eight channels with maximum stimulus current, given that the microstimulator dissipates 3.5 µW per channel for such stimulation at a rate of 33 Hz. However, with cortical neuronal firing rates of <150 spikes per second, the silicon area of the proposed converter can be reduced by ~63%.

The power pie-chart is generated assuming biphasic stimulation at a rate of 33 Hz (anodic: 94.5 µA, 192 µs; cathodic: 31.5 µA, 576 µs) and recording bandwidth of 525 Hz to 5.1 kHz. Excluding the FSK transmitter, the total power consumption is measured to be 375 µW for two modules with the analog recording front-end being the most

power-hungry circuit block. Based on simulation results, if we reduce the LNA bias currents to half their current values (all transistors and capacitors should also be sized down accordingly to maintain the same bandwidth), we can save up to 29% and 20% in silicon area and power consumption of the analog recording front-end, respectively. Although this would increase the LNA total input noise by ~41% to 4.8 μV_{rms}, it is still less than the background noise of the recording site (5 to 10 µV). Another effective approach to reduce the front-end power consumption and silicon area is to reduce the successive approximation register analog-to-digital converter (SAR ADC) resolution to 9 bits. In the proposed design, the input-referred quantization noise of the SAR ADC ($V_{DD}/(\sqrt{12} \times Gain \times 2^{ENOB})$) is ~0.8 μV_{rms} for a nominal gain of 60 dB, which is much less than that of the LNA (~3 μV_{rms}). Therefore, reducing the SAR ADC resolution by one bit would not degrade the performance considerably. Further, the power consumption of the secondary amplifier (~17% of the total system power) driving the capacitive network of the ADC can be significantly reduced as well by decreasing the ADC resolution.

Example 2

This example presents experimental results from biological tests with anesthetized and ambulatory rats using a neural prosthetic device of the present disclosure. The experiments were conducted in the cerebral cortex of adult Long-Evans rats in accordance with guidelines approved by the Institutional Animal Care and Use Committee, Kansas University Medical Center, Kansas City, Kans.

FIG. 13 is an illustration of the experimental setup for this example, using spike-triggered ICMS in an ambulatory rat. An ASIC as depicted in FIGS. 14 and 15, together with a minimum number of external components and a single coin battery (1.55 V), were assembled on a rigid-flex substrate to create a miniature, head-mounted microdevice. Neural data were transmitted wirelessly via a radio-frequency frequency-shift-keyed (RF-FSK) link at ~433 MHz between the microdevice and a commercial RF receiver (AOR, Torrance, Calif.), which down-converts the RF signal to an intermediate frequency (IF) of 10.7 MHz. A wired connection was temporarily attached to the microdevice for programming and monitoring its operation status. A custom external receiver board was used for signal conditioning and decoding of wired and wireless signals. A digital data acquisition (DAQ) card (National Instruments, Austin, Tex.) established a high-speed connection between the receiver board and a PC used for microdevice programming as well as storage and analysis of the recorded data with MAT-LAB™.

ASIC Overview

FIG. 14 depicts a block diagram and a die micrograph of a 0.35-µm two-poly four-metal (2P/4M) complementary metal-oxide-semiconductor (CMOS) integrated circuit used in this example. Each four-channel module of the integrated circuit incorporates a recording front-end, a digital signal processing (DSP) unit, and a stimulating back-end. For autonomous operation from a single 1.55-V battery, the ASIC also integrated a dc-dc converter that generated 5 V from the battery as the power supply for the stimulating back-end. It was capable of delivering ICMS sequences via an external trigger as well as triggered by neural spikes discriminated in real time, with precise control over the stimulation time instance. The recording front-end featured a bandpass frequency response with the low and high cutoff frequencies programmable from 1.1 to 525 Hz and 5.1 to 12

kHz, respectively, and provided 2b-programmable ac amplification (nominal gain of ~60 dB at 1 kHz), dc input stabilization, and 10b digitization of the recorded neural signals.

The DSP unit used in each module provided additional digital highpass filtering to remove any residual dc offsets or low-frequency artifacts and subsequently performed real-time spike discrimination based on threshold crossing and two user-adjustable time-amplitude windows. The digital highpass filter (HPF) used in the DSP unit had a programmable cutoff frequency of 366 or 756 Hz, given a 1-MHz system clock. If a spike event was accepted on any channel, the corresponding spike discriminator output (SDO) was activated after a programmable time delay (0 to ~28.6 ms).

The decision circuitry then generated any logic combination of SDO 1~4 as a trigger signal for stimulation activation. Upon triggering, the programmable stimulating backend delivered a charge-balanced asymmetric biphasic stimulus or monophasic stimulus with passive discharge to the neural tissue. The anodic and cathodic current pulse amplitudes were 6b-programmable from 0 to 94.5 μA and 31.5 μA, respectively. With a 1-MHz system clock, the duration of the anodic phase could be programmed from 0 to 240 μs with a resolution of 16 μs, whereas that of the cathodic phase was programmable from 0 to 720 μs with a resolution of 1 μs. For monophasic stimulation, the duration of the constant-current phase was programmable from 0 to 1.008 ms with a resolution of 16 μs. Passive discharge was performed after each constant-current phase to drain the accumulated charge on the stimulation site via a 2b-programmable resistor.

In constructing the head-mounted microdevice, one four-channel module of the ASIC was used for spike-triggered ICMS. Further, in the nominal operating condition of the ASIC, the bandwidth of the recording front-end was set to be 525 Hz to 5.1 kHz and the cutoff frequency of the digital HPF was set to 366 Hz. The stimulating back-end was also programmed to deliver a single monophasic current pulse (duration of 192 μs) with variable amplitude followed by passive discharge, upon receiving an external or neural-based stimulus trigger.

FIG. **15** shows the block diagram and a photograph of the assembled microdevice used in this example with an ambulatory rat. Various components were assembled on a four-layer rigid-flex printed-circuit board (PCB) made from FR-4 and polyimide (Flexible Circuit Technologies, Plymouth, Minn.). The microdevice was connected to two chronically implanted recording and stimulation microelectrodes via two microconnectors (Omnetics Corporation, Minneapolis, Minn.) in plug-and-play fashion. The microelectrodes were not permanently connected to the microdevice in order to allow replacement of the microdevice in case of failure or for reuse in additional experiments. The flexible polyimide interconnect between the microelectrode connectors and the rigid substrate allowed for some adjustability in microelectrode placement during implantation, simplifying the surgical procedure. For safe operation, four dc-blocking capacitors (220 nF) were placed in series with the stimulation channels to prevent any net dc current flow into the tissue, potentially arising from semiconductor failure or charge imbalance. A 6.8-mm, 1.55-V, silver-oxide, coin battery with capacity of 26 mAh (Energizer, St. Louis, Mo.) was selected to power the microdevice due to its small size and stable output voltage. The onboard battery powered the device continuously at its nominal operating condition for 24 hours.

A low-power, low-voltage, commercial microcontroller (ST Microelectronics, Geneva, Switzerland) programmed

the ASIC during power-up and then shut down to reduce the static power consumption. The ASIC checked the validity of the programming parameters using two 10b redundant codes. If both codes in the parameter data stream were equal to those hardwired inside the chip, the Check signal was activated; otherwise, the ASIC sent an interrupt signal to the microcontroller to turn it back on for reprogramming. A new parameter data stream could be sent to the microcontroller from the PC via the external receiver board using a bidirectional RS232 asynchronous serial link. The data were saved inside the microcontroller EEPROM and then shifted into the chip. Once ASIC programming was successful, the microcontroller transmitted an acknowledgment signal back to the PC.

The FSK wireless link in the microdevice could transmit either the full-voltage record on one channel or spike discrimination events on all four channels to the RF receiver placed as far as 2 m from the rat. A 5-cm twisted wire was used as the antenna connected to one side of an external resonant inductor (33 nH)-capacitor (3.9 pF) LC tank. These LC components resulted in an RF link frequency of ~433 MHz, given a tolerance of 5% in their values and parasitic contribution by input-output (I/O) pads, wire bonds, and PCB interconnects. The wireless recording of broad-band neural data was limited in this example to a single channel due to battery lifetime considerations for supporting higher data rates. Nonetheless, the raw data recorded on all four channels of the microdevice could still be accessed simultaneously using a wired link between the microdevice and the external receiver board. The wired connection also can provide the output voltage level on all four stimulation channels to monitor stimulation site impedance during long-term experiments.

A commercial low-dropout (LDO) voltage regulator (ST Microelectronics, Geneva, Switzerland) together with four external capacitors were used to isolate the power supply line of the sensitive front-end recording circuitry from that of the rest of the system, mainly the noisy digital circuitry and 1.5-to-5V converter. Given the non-zero source impedance of the silver-oxide coin battery (5 to 10Ω), this scheme was critical to ensure robust, reliable operation of the sensitive recording front-end. Although the power supply rejection ratio (PSRR) of the recording front-end was measured to be >65 dB, this measurement is typically done with the input shorted to ground. As depicted schematically in FIG. **16**, the combination of the recording microelectrode capacitance C_E and parasitic capacitors $C_{P1,2}$ in the analog I/O block contributed by electrostatic discharge protection circuitry and bonding pad created an additional signal path for the supply-induced noise that can degrade the PSRR in practice. From FIG. **16**, the PSRR through I/O parasitic capacitors could be derived as

$$PSRR_{I/O} = \frac{C_E + C_{p1} + C_{p2} + C_{IN}}{C_{P1}} \cong \frac{C_{IN} + C_E}{C_{P1}}$$

where C_{IN} is the input capacitance of the recording front-end, which is 28 pF in this example. Given C_E of 150 pF (i.e., recording site impedance of ~1.1 MΩ at 1 kHz) and estimated values of 1 pF for $C_{P1,2}$, the above equation results in $PSRR_{I/O}$ of 45 dB. FIG. **16** also shows the measured PSRR with V_{IN} shorted to ground as well as that with V_{IN} connected to ground via a 150-pF external capacitor. $PSRR_{I/O}$ was measured to be ~44 dB at 1 kHz, in good agreement with the above equation. Therefore, measured

noise of 10 mV$_{pp}$ on the battery voltage would induce ~63-μV$_{pp}$ noise on the input, greatly degrading the recording signal-to-noise ratio. Instead, the LDO regulator attenuated the power supply noise by more than 60 dB at 1 kHz, reducing the noise induced on the input well below the thermal and flicker noise levels of the recording front-end.

External Receiver Board

FIG. **17** shows the block diagram and a photograph of the custom external receiver board used in this example. It incorporated FSK demodulation circuitry using a commercial phase-locked loop device (NXP Semiconductors, The Netherlands), which detected the frequency variation of the amplified/filtered 10.7-MHz IF signal for further down-conversion to baseband. The wirelessly received data together with four channels of wired data were processed in a complex programmable logic device (Altera, San Jose, Calif.), which used a Manchester decoder for clock/data recovery and sent the signals to the PC via the DAQ card. Any one of the five data channels could be selected by the user for broadcasting of the data stream through a speaker. Specifically, a preamble detector and a deserializer unit convert the selected data stream to 10b digital codes that are then converted to an analog audio signal using a digital-to-analog converter (Analog Devices, Norwood, Mass.). This feature allowed a trained user to rapidly identify whether neural activity was present in the recorded data stream by listening to the sound of spiking neurons. The onboard microcontroller unit received parameter data for microdevice operation from the PC and sent them to the microdevice via a RS232 asynchronous serial link. As stated previously, if ASIC programming is successful, the microcontroller receives an acknowledgment signal from the microdevice and then sends the programming status back to the PC.

Experiments with Anesthetized Rats

Microelectrodes were acutely implanted in two spatially separated forelimb motor areas of the rat's brain that are reciprocally connected with one another. Specifically, a micromachined silicon microelectrode with recording sites of iridium (NeuroNexus Technologies, Ann Arbor, Mich.) with impedance values of 2 to 3 MΩ was implanted in the rostral forelimb area (RFA) within the premotor cortex, and a tungsten, matrix, stimulation electrode (FHC, Bowdoin, Me.) with impedance value of 50 to 100 kΩ was implanted in the caudal forelimb area (CFA) within the primary motor cortex. Each electrode was externally interfaced with a single data channel of the recording front-end and stimulating back-end on the ASIC. A connection to the animal tail was tied to the system ground and used as a reference electrode for both recording and stimulation. In the first experiment, the CFA was stimulated at 2 Hz with a single monophasic current pulse [90 μA, 192 μs, see FIG. **18**(*a*)], using an external trigger signal. FIG. **18**(*b*) shows three traces of the recorded data from the RFA, depicting stimulus artifacts with duration of ~4 ms and four neural spikes detected by the ASIC shortly after stimulation. FIG. **18**(*c*) shows the raster plot and peristimulus histogram of the neural response to ICMS for a total of 315 ICMS pulses, depicting a clear increase in neural activity 7.5 ms after stimulation. This example demonstrates, inter alia, the system capability for simultaneous stimulation and recording the neural response to ICMS.

In a second acute experiment, neural activity was recorded on all four channels of the ASIC front-end to perform multichannel spike-triggered ICMS. If a spike event was accepted on any channel, the corresponding SDO was activated for 10 ms after a time delay of 5 ms. The decision circuitry was programmed to trigger ICMS whenever neural

activity was simultaneously present on channels 2 and 3. FIG. **19** shows the simultaneously recorded data on each channel at the output of the digital HPF along with the corresponding SDO and the resulting stimulus trigger signal during a 300-ms time window. Two large stimulus artifacts were distinguishable on each channel as a result of spike-triggered stimulation, when simultaneous spike events (within a 10-ms window) occurred on channels 2 and 3. The data in both acute experiments were recorded via the wired link.

Experiments with Ambulatory Rats

Two micromachined silicon microelectrodes (NeuroNexus Technologies, Ann Arbor, Mich.) were chronically implanted in the RFA and second somatosensory area (SII) of the rat's brain for recording and stimulation, respectively, using standard neurosurgical techniques. The recording microelectrode had sixteen 413-μm^2 iridium sites uniformly placed along the length of its 3-mm silicon shank. The stimulation electrode had sixteen 1250-μm^2 sites uniformly placed along its 2-mm shank. The stimulation sites were also activated with iridium oxide (IrO) to further reduce the site impedance to ~60-120 kΩ. A stainless steel threaded rod was mounted through an opening in the skull and affixed to it with acrylic. As shown in FIG. **20**, the microdevice was mounted ~1 cm above the rat's head and affixed to the skull using the threaded rod and nut, in such a way that the rat could not reach the microdevice. The threaded rod was also tied to the system ground and used as a reference electrode for both recording and stimulation.

Spontaneous neural activity was recorded on two of the four recording channels (Channels 3 and 4). The top two plots in FIG. **21** depict the data recorded at the output of the digital HPF within a 3-s window, and the bottom two plots depict the superimposed, time-aligned spike waveforms that crossed the user-positioned 20-μV threshold level (red dashed line). The accepted spikes (indicated with blue markers in top and as dark gray in bottom plots) also passed through the two time-amplitude window discriminators (solid red boxes), whereas the waveforms in light gray were rejected by the spike discriminator (i.e., not used for stimulus triggering).

The microdevice was programmed to trigger ICMS on all four stimulation channels using accepted spikes recorded on channel 4. Upon each trigger, the microdevice delivered a single monophasic current pulse (30 μA, 192 μs) with passive discharge to stimulate the target cortical tissue. The DSP operation was also blanked for ~28.5 ms after each spike discrimination (i.e., neural spikes on channel 4 did not trigger ICMS during this period). FIG. **22** shows the superimposed spike waveforms and corresponding stimulus artifacts from single-pulse stimulation with spike-stimulus delays of 5 and 7.5 ms. The data were recorded wirelessly as the microdevice operated autonomously from a single 1.55-V battery.

The recorded data from channels 3 and 4 (corresponding to the spike-stimulus delay case of 7.5 ms) were further analyzed to investigate whether spike-triggered ICMS induced any electrophysiological change in the cortical circuitry. This was intended to show the physiological effect of the stimulating electrode beyond simply showing the stimulus artifact. The top left plot in FIG. **23** depicts a 34-ms window of the recorded data on channel 4, showing the trigger spike, the resulting stimulus artifact, and three other spikes that occurred during the DSP blanking period (indicated by red markers). The middle left plot depicts the peristimulus histogram (1-ms bins) during the DSP blanking period for 3600 trials. The trigger spikes occurred just prior

to the start of the histogram. The histogram suggests that the neuronal firing rate after ICMS was lower than that prior to stimulation. A paired T-test also confirmed that the reduction of the neuronal firing rate after ICMS was statistically significant with p<0.0001. The bottom left plot depicts the mean neuronal firing rate (±99% confidence interval) before and after ICMS on channel 4. The same effect was also observed on channel 3 as shown in the plots on the right, although generally fewer spikes were recorded on that channel throughout the experiment.

To determine whether the firing rate returned to baseline levels after the cessation of stimulation, the effect of spike-triggered ICMS over a much longer time scale was examined, beginning ~90 s before stimulation, then during the 500-s stimulation period, and for ~410 s after stimulation (see FIG. 24.) The top plot depicts the measured stimulation rate versus time, whereas the middle and bottom plots depict the mean neuronal firing rate on channels 3 and 4, respectively. The data were smoothed by applying a moving average with a 25-s time window. The dashed lines show the average level for each section of the plot in time. FIG. 24 clearly shows that the neuronal firing rate not only decreases during spike-triggered ICMS, but also that it returns to the pre-stimulus level once ICMS is terminated.

Further, as expected, the stimulation rate is slightly below the neuronal firing rate on channel 4 during ICMS, because the spike events on channel 4 that occur during the DSP blanking period do not trigger stimulation. The reduction in spiking rate of channel 4 (and to a lesser extent, channel 3) is likely the result of activating horizontal connections that project from the point of stimulation to the recording site. These projections can innervate inhibitory interneurons that, when activated, would lead to a reduction of the activity of the recorded neurons.

Example 3

Methods

Animals

Fifteen Male Long-Evans rats (350-450 g) were obtained from Harlan. At approximately four months of age, animals were randomly assigned to one of three groups: activity-dependent stimulation (ADS; n=6), randomized open-loop stimulation (OLS; n=5), or no stimulation (Control; n=5). Rats were housed individually and were maintained on a 12:12 h light:dark cycle. Rat chow was provided (3-5% body weight) on a feeding schedule to promote compliance on behavioral tasks and was supplemented with rodent food pellets during the skilled reaching task. Protocols for animal use were approved by the University of Kansas Medical Center Institutional Animal Care and Use Committee (IACUC) and adhered to the Guide for the Care and Use of Laboratory Animals (National Research Council, 1996).

Behavioral Training

Skilled Reach Test.

Each animal was put into a Plexiglas reaching chamber and a single banana-flavored food pellet (45 mg, Bioserv) was placed into a shallow food well 2 cm from the front wall on an external shelf positioned 3 cm from the bottom of a 10-in^3 chamber (Withers and Greenough, 1989; Bury and Jones, 2002; Hsu and Jones, 2005). The opening of the chamber was such that only the left forelimb could be used for reaching. Prior to entry into the remainder of the study, the animal was required to reach and retrieve food pellets above 70% success for three consecutive days. The percentage of successful retrievals was based on the number of

successful pellets grasped, retrieved, and brought to the animal's mouth during a total of 60 trials. Probe trials occurred on Days 3, 5, 8, 14 and 21 following an infarct within the forelimb motor area of the cerebral cortex and consisted of 20 trials with microdevice stimulation on and 20 trials with microdevice stimulation off.

Surgical Procedures

Animals were initially anesthetized with ketamine (100 mg/kg i.p.) and xylazine (5 mg/kg i.m.), prior to being placed within a stereotaxic frame, and given supplements of ketamine (20 mg/kg i.m.) during the surgical procedure as needed. A midline incision was made to expose the skull surface, then a 5-mm trephine hole was made over the right hemisphere using stereotaxic coordinates to expose the CFA centered at +0.5 mm rostral, +2.5 mm lateral relative to bregma. Two 1-mm burr holes were made over a secondary motor area, the RFA, and the hand area of primary somatosensory cortex (S1) in the right hemisphere using corresponding stereotaxic coordinates (+3.5, +2.5 and −1.25, +4.25, respectively). Three additional burr holes (0.625 mm) were made for skull screws, one along the lateral ridge on either parietal bone, and one in the center of the interparietal bone. The dura was resected over S1 and RFA, but left intact over CFA.

Defining Physiological Areas

The RFA and S1 areas were isolated using electrophysiological mapping techniques. Burr holes over each area allowed up to 12 sites to be tested at 250-μm resolution. To verify the RFA, a 16-channel Michigan electrode (NeuroNexus Technologies) was inserted into the burr hole to a depth of 1700 μm and intracortical microstimulation was delivered as a 40-ms train of thirteen, 0.2-ms monophasic cathodal pulses delivered at 333 Hz at the rate of one train per second (TDT). During stimulation, the current delivered was gradually increased from 1 μA to 80 μA. Upon stimulation, the animal was visually observed for evoked movements. Forelimb movements that were bounded caudally by neck/trunk responses were considered within RFA. To verify S1, a Michigan electrode was inserted into the burr hole and the neural signal was amplified and fed into a speaker and a digital display. The left forelimb was palpated until the touching could be correlated with both the amplified sound of the neural activity and spikes on the display (TDT). The hand area of S1 was defined by evoked responses that could be localized to cutaneous stimulation of the wrist, hand, or digit. Both RFA and S1 were found in each animal before proceeding with the cortical impact.

Cortical Impact

After defining RFA and S1, a controlled cortical impact was delivered to CFA using the Impact One stereotaxic impactor (Leica Microsystems). The impact was delivered via a flat, circular tip with a 3-mm diameter. The impactor tip was fully extended and then slowly lowered onto the surface of the dura. Contact with the dura was indicated by an audio signal triggered by a feedback sensor. The impactor tip was then retracted within the impactor arm, and the arm was then lowered 2 mm. Once triggered, the impactor tip accelerated at 1.5 m/s extending 2 mm below the surface of the dura. The impactor tip remained extended for 100 ms then automatically retracted, leaving the dura intact.

Microdevice Implantation

Following the impact, skull screws were implanted into the parietal bones, and a threaded rod was implanted into the interparietal bone. These were affixed to the skull with dental acrylic. A hybrid, 16-channel, chronic Michigan probe for recording was inserted into the area defined as RFA using a micropositioner. The probe and burr hole

opening were then sealed with a silicone polymer (Kiwk-Cast, WPI). The base of the probe connector was lowered onto the dental acrylic and fixed into place. An activated, 16-channel, chronic Michigan probe for stimulation was inserted into the area defined as S1 hand area and fixed into place in the same manner as above. Any remaining exposed areas were covered with the silicone polymer before suturing the incision. The microdevice was then affixed to the threaded rod with stainless steel nuts and spacers, and its connectors plugged into those of the appropriate electrodes. Technical aspects of the microdevice were described elsewhere (Azin et al., 2011a,b), but in short, the microdevice was able to autonomously record from up to four of the 16 channels of the recording microelectrode located in RFA, amplify and digitize the neural signals, and employ a user-programmable spike discrimination algorithm to trigger activity-dependent stimulation pulses delivered to the microelectrode implanted in S1 hand area.

Electrophysiological Recording

Initial Programming.

Two to four hours following the microdevice implantation, a 1.55-V battery was inserted into the microdevice. An Omnetics connector leading to a custom-built controller board was plugged into the microdevice, and the microdevice was initially programmed to record on all four available channels. Signals from these four channels were recorded from the microdevice and routed through the controller board to a LabVIEW data acquisition card. The signals were monitored in real time through both software and an amplified audio signal from the controller board. The highpass-filtered signal from one of the four channels was exported to MATLAB™ and loaded into a spike discrimination script within MATLAB™. A threshold level was defined above the noise level of the signal, and small segments of waveforms that crossed the threshold level were overlaid on each other at the threshold crossing point. Spikes were then defined by two user-adjustable time-amplitude windows, with the priority of maximizing detection of observed spikes while avoiding noise and/or stimulus artifacts. Once the spike discrimination parameters were defined, they were imported into the microdevice programming software. Stimulation parameters were also set in the software to a 60-μA current delivered pseudo-biphasically with pulse duration of 192 μs. For the ADS group, stimulation was set to occur 7.5 ms following spike discrimination on the channel from which the parameters were derived. For the OLS group, stimulation current and pulse duration were the same as for the ADS group, and pulses were pseudo-biphasic. However, the stimulator was not dependent upon recorded signals in RFA. Instead, the stimulation occurred independently throughout the post-lesion period with inter-stimulus intervals ranging from 35 to 200 ms. This range of inter-stimulus intervals was derived from prior data using ADS and corresponded with the most common range of stimulation frequencies of the ADS group. Any individual inter-stimulus interval (and hence, frequency of stimulation) chosen was randomized equally across the range to more closely approximate the level of stimulation the ADS group received.

Finally, the output was programmed to transmit the data through either a wired connection or a wireless connection. The microdevice was reprogrammed and additional recordings were taken to assess the spike discrimination parameters. The microdevice was then programmed to transmit the data wirelessly, and the animal was allowed to move freely about its cage.

Signal Maintenance.

The microdevice consumed power at a level to necessitate battery changes once daily for ADS and twice daily for OLS groups. Each animal's microdevice was tested a minimum of once a day to confirm its functionality. Occasionally, there was a discrepancy between spikes observed on the monitoring software and spikes actually being detected. When this occurred, the microdevice was reconnected to the wired connection, the stimulation was turned off, and the activity was processed through the spike discrimination software. In order to maximize spike discrimination, the threshold and/or time-amplitude windows were slightly adjusted to compensate for detection failures. If no spiking was detected, the remaining channels were monitored. If there was signal on one or more of the remaining channels, the stimulation trigger was moved to the most active channel. If no activity was detected on all four channels, the microdevice was removed and the microelectrodes were tested with commercial electrophysiology equipment (TDT). If the electrodes were still functional and the animal had not fully recovered from the injury, a new microdevice was attached to the animal and reprogrammed as above.

Behavioral Tasks.

During behavioral tasks, the microdevice was reprogrammed so that one half of each behavioral trial was done while the microdevice stimulator was turned on and the other half was done while the stimulator was turned off. Control animals were given equivalent time and trials on the tasks. Except for signal maintenance and dead batteries, this was the only time that the ADS and OLS groups were not receiving stimulation.

Data Recording.

The highpass-filtered neural signal was recorded at ~35 kHz from either one or four channels (wireless or wired connection, respectively) during all signal monitoring and behavioral trials using LabVIEW software. In addition, all animals had multiple sessions where data were recorded during home cage behavior. The raw signal recording duration of any single trial was software limited to ~45 min, but the spiking time stamp data could be recorded for up to 24 hours. The neural signal data were converted from a LabVIEW file to a text file and analyzed using custom MATLAB™ software.

Results

The results demonstrated a potent and statistically significant effect of ADS on motor performance after only 8 days of operation. By Day 14 post-lesion, performance in the ADS group was indistinguishable from pre-lesion performance (~70% with stimulation "on" based on linear mixed model, intent-to-treat design; FIG. 25A). The improvement persisted at Day 21 post-injury. In the ADS group, performance in the stimulation on condition increased from 27% on Day 3 post-injury to 39% on Day 5 post-injury, 53% on Day 8 post-injury, and 69% on Day 14 post-injury. The improvement in performance was also evident in the stimulation off condition in the ADS group, and was statistically significant on Days 8, 14 and 21 post-injury.

In contrast, while there was some improvement in the OLS group (statistically significant difference from control animals on Day 21 post-injury; FIGS. 25A and 25B), effects were reduced compared to the ADS group. By Day 14 post-injury, performance was 45% and, based on modeled data, never exceeded 50% in either stimulation on or off conditions. Untreated control animals performed at <25% throughout the recovery period.

Further, there were substantial differences between the on and off states of the microdevice operation during behavioral testing (FIG. **26**). In the ADS group, the animals were up to 13% better with the device stimulation on vs. off (FIG. **26**). These differences were evident in the ADS group until Day 21 post-injury, when on vs. off states were similar. In individual rats, these differences were quite pronounced on specific days, especially on Days 5 and 8 post-injury. As an example, in one rat on Day 8 post-injury, the difference between the on vs. off states was over 40%, with twice as many pellets retrieved during the on state.

In the OLS group, rats performed slightly worse with the stimulation turned on vs. off (FIG. **26**), but this difference never exceeded 7% (Day 3 post-injury). However, some rats performed substantially worse with the stimulation turned on vs. off (Day 3, 14 and 21).

Discussion

The results demonstrate, inter alia, that ADS between the spared premotor cortex (i.e., the RFA) and the somatosensory hand area can result in a rapid improvement in motor function by Day 8 post-lesion, and that the improved function persists through at least Day 21 post-lesion. This is the first demonstration that ADS can be used to positively affect function after cortical injury.

One of the many advantages of the present disclosure is that, in some embodiments, it may provide for a cortical communication bridge allowing distant cortical areas with substantially no effective communication to be artificially linked after injury, which may have widespread clinical application. The results shown in Example 3 demonstrate, inter alia, that somatosensory-motor communication links that are disrupted following TBI can be restored by a microdevice of the present disclosure, thereby promoting restoration of functional movements. It is possible that a microdevice of the present disclosure may also be applied to sensorimotor dysfunction after stroke. It is also possible that a microdevice of the present disclosure may also be applied to certain aphasic conditions after either stroke or TBI. Neuroimaging studies in humans have shown that the arcuate fasciculus connecting Broca's and Wernicke's areas in the brain is altered with specific types of training (Schlaug et al., 2009). It may be possible to use the methods and devices of the present disclosure to automatically aid in the reconnection of this functionally important communication link in the brain to restore language. In addition, there are several neurological and psychiatric disorders that include what has broadly been termed "disconnection syndromes" that could be aided by the methods and devices of the present disclosure. In some embodiments, it is also possible that a microdevice of the present disclosure may provide for a neural communication bridge in cortex or subcortical structures to alleviate functional disorders in idiopathic conditions, i.e., when specific dysfunctional communication cannot be identified. Finally, in some embodiments, it is also possible that a microdevice of the present disclosure may provide for a neural communication bridge in cortex or subcortical structures to improve function or behavioral performance in otherwise healthy brains.

Therefore, the present invention is well adapted to attain the ends and advantages mentioned as well as those that are inherent therein. The particular embodiments disclosed above are illustrative only, as the present invention may be modified and practiced in different but equivalent manners apparent to those skilled in the art having the benefit of the teachings herein. Furthermore, no limitations are intended to the details of construction or design herein shown, other than as described in the claims below. It is therefore evident that

the particular illustrative embodiments disclosed above may be altered or modified and all such variations are considered within the scope and spirit of the present invention. While compositions and methods are described in terms of "comprising," "containing," or "including" various components or steps, the compositions and methods can also "consist essentially of" or "consist of" the various components and steps. All numbers and ranges disclosed above may vary by some amount. Whenever a numerical range with a lower limit and an upper limit is disclosed, any number and any included range falling within the range is specifically disclosed. In particular, every range of values (of the form, "from about a to about b," or, equivalently, "from approximately a to b," or, equivalently, "from approximately a-b") disclosed herein is to be understood to set forth every number and range encompassed within the broader range of values. Also, the terms in the claims have their plain, ordinary meaning unless otherwise explicitly and clearly defined by the patentee. Moreover, the indefinite articles "a" or "an," as used in the claims, are defined herein to mean one or more than one of the element that it introduces. If there is any conflict in the usages of a word or term in this specification and one or more patent or other documents that may be incorporated herein by reference, the definitions that are consistent with this specification should be adopted.

REFERENCES

1. M. M. Ahmadi, "A new modeling and optimization of gain-boosted cascode amplifier for high-speed and low-voltage applications," *IEEE Trans. Circuits Syst. II*, vol. 53, no. 3, pp. 169-173, March 2006.
2. A. T. Avestruz, W. Santa, D. Carlson, R. Jensen, S. Stanslaski, A. Helfenstine, and T. Denison, "A 5 µW/channel spectral analysis IC for chronic bidirectional brain-machine interfaces," *IEEE J. Solid-State Circuits*, vol. 43, no. 12, pp. 3006-3024, December 2008.
3. M. Azin, D. J. Guggenmos, S. Barbay, R. J. Nudo, and P. Mohseni, "A battery-powered activity-dependent intracortical microstimulation IC for brain-machine-brain interface," *IEEE J. Solid-State Circuits*, vol. 46, no. 4, April 2011, In Press.
4. M. Azin, D. J. Guggenmos, S. Barbay, R. J. Nudo, and P. Mohseni, "An activity-dependent brain microstimulation SoC with integrated 23 nV/rtHz neural recording front-end and 750 nW spike discrimination processor," in *IEEE Symp. VLSI Circuits Dig. Papers*, Honolulu, Hi., Jun. 16-18, 2010, pp. 223-224.
5. M. Azin and P. Mohseni, "A high-output-impedance current microstimulator for anatomical rewiring of cortical circuitry," in *Proc. IEEE Int. Symp. Circuits and Systems (ISCAS'08)*, Seattle, Wash., May 18-21, 2008, pp. 2502-2505.
6. T. W. Berger et al., "Restoring lost cognitive function: Hippocampalcortical neural prostheses," *IEEE Eng. Med. Biol. Mag.*, vol. 24, no. 5, pp. 30-44, September/October 2005.
7. P. K. Campbell, K. E. Jones, R. J. Huber, K. W. Horch, and R. A. Normann, "A silicon-based, three-dimensional neural interface: Manufacturing process for an intracortical electrode array," *IEEE Trans. Biomed. Eng.*, vol. 38, pp. 758-767, 1991.
8. M. S. Chae, Z. Yang, M. R. Yuce, L. Hoang, and W. Liu, "A 128-channel 6-mW wireless neural recording IC with spike feature extraction and UWB transmitter," *IEEE Trans. Neural Syst. Rehab. Eng.*, vol. 17, no. 4, pp. 312-321, August 2009.

9. T. Chen, K. Chen, Z. Yang, K. Cockerham, and W. Liu, "A biomedical multiprocessor SoC for closed-loop neuroprosthetic applications," in *IEEE Int. Solid State Circuits Conference (ISSCC'09) Dig. Tech. Papers*, San Francisco, Calif., Feb. 8-12, 2009, pp. 434-435.

10. T. G. Constandinou, J. Georgiou, and C. Toumazou, "A partial-current-steering biphasic stimulation driver for vestibular prostheses," *IEEE Trans. Biomed. Circuits Syst.*, vol. 2, no. 2, pp. 106-113, June 2008.

11. T. Denison, K. Consoer, W. Santa, A.-T. Avestruz, J. Cooley, and A. Kelly, "A 2 W 100 nV/rtHz chopper-stabilized instrumentation amplifier for chronic measurement of neural field potentials," *IEEE J. Solid-State Circuits*, vol. 42, no. 12, pp. 2934-2945, December 2007.

12. X. J. Feng, B. Greenwald, H. Rabitz, E. Shea-Brown, and B. Kosut, "Toward closed-loop optimization of deep brain stimulation for Parkinson's disease: Concepts and lessons from a computational model," *J. Neural Eng.*, vol. 4, pp. L14-21, 2007.

13. M. Ghovanloo and K. Najafi, "A compact large-voltage-compliance high-output-impedance programmable current source for implantable microstimulators," *IEEE Trans. Biomed. Eng.*, vol. 52, no. 1, pp. 97-105, January 2005.

14. R. R. Harrison and C. Charles, "A low-power low-noise CMOS amplifier for neural recording applications," *IEEE J. Solid-State Circuits*, vol. 38, no. 6, pp. 958-965, June 2003.

15. L. R. Hochberg, M. D. Serruya, G. M. Friehs, J. A. Mukand, M. Saleh, A. H. Caplan, A. Branner, D. Chen, R. D. Penn, and J. P. Donoghue, "Neuronal ensemble control of prosthetic devices by a human with tetraplegia," *Nature*, vol. 442, pp. 164-171, July 2006.

16. A. Jackson, J. Mavoori, and E. E. Fetz, "Long-term motor cortex plasticity induced by an electronic neural implant," *Nature*, vol. 444, pp. 56-60, November 2006.

17. A. Jackson, C. T. Moritz, J. Mavoori, T. H. Lucas, and E. E. Fetz, "The neurochip BCI: Towards a neural prosthesis for upper limb function," *IEEE Trans. Neural Syst. Rehab. Eng.*, vol. 14, no. 2, pp. 187-190, June 2006.

18. A. Keller and H. Asanuma, "Synaptic relationships involving local axon collaterals of pyramidal neurons in the cat motor cortex," *J. Comp. Neurol.*, vol. 336, pp. 229-242, 1993.

19. J. Lee, H. G. Rhew, D. R. Kipke, and M. P. Flynn, "A 64-channel programmable closed-loop neurostimulator with 8-channel neural amplifier and logarithmic ADC," *IEEE J. Solid-State Circuits*, vol. 45, no. 9, pp. 1935-1945, September 2010.

20. X. Liu, A. Demosthenous, and N. Donaldson, "An integrated implantable stimulator that is fail-safe without off-chip blocking capacitors," *IEEE Trans. Biomed. Circuits Syst.*, vol. 2, no. 3, pp. 231-244, September 2008.

21. J. Mavoori, A. Jackson, C. Diorio, and E. Fetz, "An autonomous implantable computer for neural recording and stimulation in unrestrained primates," *J. Neurosci. Methods*, vol. 148, pp. 71-77, 2005.

22. D. J. McFarland and J. R. Wolpaw, "Brain-computer interface operation of robotic and prosthetic devices," *Computer*, vol. 41, no. 10, pp. 52-56, October 2008.

23. M. Mollazadeh, K. Murari, G. Cauwenberghs, and N. Thakor, "Micropower CMOS-integrated low-noise amplification, filtering, and digitization of multimodal neuropotentials," *IEEE Trans. Biomed. Circuits Syst.*, vol. 3, no. 1, pp. 1-10, February 2009.

24. C. T. Moritz, S. I. Perlmutter, and E. E. Fetz, "Direct control of paralyzed muscles by cortical neurons," *Nature*, vol. 456, pp. 639-643, 2008.

25. M. A. L. Nicolelis, A. A. Ghazanfar, B. M. Faggin, S. Votaw, and L. M. O. Oliveira, "Reconstructing the Engram: Simultaneous, multisite, many single neuron recordings," *Neuron*, vol. 18, pp. 529-537, April 1997.

26. M. Nishibe, S. Barbay, D. Guggenmos, and R. J. Nudo, "Reorganization of motor cortex after controlled cortical impact in rats and implications for functional recovery," J. Neurotrauma, vol. 27, pp. 2221-2232, December 2010.

27. M. Ortmanns, A. Rocke, M. Gehrke, and H. J. Tiedtke, "A 232-channel epiretinal stimulator ASIC," *IEEE J. Solid-State Circuits*, vol. 42, no. 12, pp. 2946-2959, December 2007.

28. J. P. Rauschecker and R. V. Shannon, "Sending sound to the brain," *Science*, vol. 295, no. 5557, pp. 1025-1029, February 2002.

29. F. Shahrokhi, K. Abdelhalim, D. Serletis, P. L. Carlen, and R. Genov, "The 128-channel fully differential integrated neural recording and stimulation interface," *IEEE Trans. Biomed. Circuits Syst.*, vol. 4, no. 3, pp. 149-161, June 2010.

30. J. J. Sit and R. Sarpeshkar, "A low-power blocking-capacitor-free charge-balanced electrode-stimulator chip with less than 6 nA dc error for 1-mA full-scale stimulation," *IEEE Trans. Biomed. Circuits Syst.*, vol. 1, no. 3, pp. 172-183, September 2007.

31. A. M. Sodagar, G. E. Perlin, Y. Yao, K. Najafi, and K. D. Wise, "An implantable 64-channel wireless microsystem for single-unit neural recording," *IEEE J. Solid-State Circuits*, vol. 44, no. 9, pp. 2591-2604, September 2009.

32. K. Sooksood, T. Stieglitz, and M. Ortmanns, "An active approach for charge balancing in functional electrical stimulation," *IEEE Trans. Biomed. Circuits Syst.*, vol. 4, no. 3, pp. 162-170, June 2010.

33. Y. Tsividis, *Operation and Modeling of the MOS Transistor,* 2nd ed. New York, N.Y.: Oxford Univ. Press, 1999.

34. B. K. Thurgood, D. J. Warren, N. M. Ledbetter, G. A. Clark, and R. R. Harrison, "A wireless integrated circuit for 100-channel charge-balanced neural stimulation," *IEEE Trans. Biomed. Circuits Syst.*, vol. 3, no. 6, pp. 405-414, December 2009.

35. M. Velliste, S. Perel, M. C. Spalding, A. S. Whitford, and A. B. Schwartz, "Cortical control of a prosthetic arm for self-feeding," *Nature*, vol. 453, pp. 1098-1101, June 2008.

36. S. Venkatraman, K. Elkabany, J. D. Long, Y. Yao, and J. M. Carmena, "A system for neural recording and closed-loop intracortical microstimulation in awake rodents," *IEEE Trans. Biomed. Eng.*, vol. 56, no. 1, pp. 15-22, January 2009.

37. R. J. Vetter, J. C. Williams, J. F. Hetke, E. A. Nunamaker, and D. R. Kipke, "Chronic neural recording using silicon-substrate microelectrode arrays implanted in cerebral cortex," *IEEE Trans. Biomed. Eng.*, vol. 51, pp. 896-904, 2004.

38. W. Wattanapanitch, M. Fee, and R. Sarpeshkar, "An energy-efficient micropower neural recording amplifier," *IEEE Trans. Biomed. Circuits Syst.*, vol. 1, no. 2, pp. 136-147, June 2007.

39. J. D. Weiland and M. S. Humayun, "Intraocular retinal prosthesis," *IEEE Eng. Med. Biol. Mag.*, vol. 25, no. 5, pp. 60-66, September/October 2006.

40. R. F. Yazicioglu, P. Merken, R. Puers, and C. Van Hoof, "A 200 μW eight-channel EEG acquisition ASIC for

ambulatory EEG systems," *IEEE J. Solid-State Circuits*, vol. 43, no. 12, pp. 3025-3038, December 2008.

41. M. Yin and M. Ghovanloo, "Using pulsewidth modulation for wireless transmission of neural signals in multi-channel neural recording systems," *IEEE Trans. Neural Syst. Rehab. Eng.*, vol. 17, no. 4, pp. 354-363, August 2009.

What is claimed is:

1. A method of using a neural prosthetic device, the neural prosthetic device comprising an integrated circuit that comprises a recording front-end which includes a plurality of recording channels, a stimulus delivering back-end which includes a plurality of stimulation channels, and a processor unit which includes a spike discriminator and decision circuitry, wherein the method comprises:

the processor unit detecting a first neural spike in at least a first channel of the plurality of recording channels at a first time value;

the processor unit detecting a second neural spike in at least a second channel of the plurality of recording channels at a second time value;

the processor unit comparing the first time value of the first neural spike from the first channel to the second time value of the second neural spike from the second channel; and

if the first time value and second time value meet a predetermined criterion, the processor unit causing a stimulus to be delivered in at least one of the plurality of stimulation channels within a defined period of time after the detection of the first and second neural spikes.

2. The method of claim 1, wherein the spike discriminator identifies acceptable neural spikes by using a spike discrimination algorithm that utilizes adjustable, user-set parameters.

3. A neural prosthetic device comprising:

an integrated circuit that comprises:

a recording front-end comprising a plurality of recording channels;

a stimulus delivering back-end comprising a plurality of stimulation channels; and

a processor unit comprising a spike discriminator and decision circuitry, the processor unit configured to:

detect a first neural spike in at least a first channel of the plurality of recording channels at a first time value,

detect a second neural spike in at least a second channel of the plurality of recording channels at a second time value,

compare the first time value of the first neural spike from the first channel to the second time value of the second neural spike from the second channel, and

if the first time value and second time value meet a predetermined criterion, cause a stimulus to be delivered in at least one of the plurality of stimulation channels within a defined period of time after the detection of the first and second neural spikes.

4. The device of claim 3, wherein the predetermined criterion comprises the first time value and second time value both occurring within a time window.

5. The device of claim 3, wherein the recording front-end is configured to detect the first neural spike at a first neural site in a functional area of a cortex, and the stimulus delivering back-end is configured to deliver the stimulus at a second neural site in a different functional area of the cortex.

6. The device of claim 3 wherein the spike discriminator identifies acceptable neural spikes by using a spike discrimination algorithm.

7. The device of claim 6 wherein the spike discrimination algorithm utilizes adjustable, user-set parameters.

8. The device of claim 3, wherein the spike discriminator includes a threshold level and a time-amplitude window.

9. The device of claim 3, wherein the stimulus is an asymmetric biphasic electrical pulse.

10. The device of claim 3, wherein the stimulus is a monophasic or biphasic electrical pulse.

11. The device of claim 3, wherein the stimulus has an intensity of ≤10 mA.

12. The device of claim 3 further comprising a recording microelectrode having a plurality of recording sites operably connected to the plurality of recording channels of the recording front-end of the integrated circuit.

13. The device of claim 3 further comprising a stimulation microelectrode having a plurality of stimulation sites operably connected to the plurality of stimulation channels of the stimulus delivering back-end of the integrated circuit.

14. The device of claim 3 further comprising a power supply operably connected to the stimulus delivering back-end.

15. The device of claim 3 wherein the processor unit is a digital signal processor unit.

16. The device of claim 3 wherein the recording front-end further comprises a low-noise amplifier, a highpass filter, a secondary amplifier and an analog-to-digital converter.

17. The device of claim 3 wherein the stimulus delivering back-end further comprises a stimulator timing control, a signal level shifter, and a digital-to-analog converter.

18. The device of claim 3 further comprising a radio-frequency transmitter.

19. One or more hardware storage devices having stored thereon computer-executable instructions that are executable by an integrated circuit of a neural prosthetic device, the integrated circuit comprising:

a recording front-end comprising a plurality of recording channels;

a stimulus delivering back-end comprising a plurality of stimulation channels; and

a processor unit comprising a spike discriminator and decision circuitry, wherein the computer-executable instructions cause the processor unit to:

detect a first neural spike in at least a first channel of the plurality of recording channels at a first time value;

detect a second neural spike in at least a second channel of the plurality of recording channels at a second time value;

compare the first time value of the first neural spike from the first channel to the second time value of the second neural spike from the second channel; and

if the first time value and second time value meet a predetermined criterion, cause a stimulus to be delivered in at least one of the plurality of stimulation channels within a defined period of time after the detection of the first and second neural spikes.

20. The one or more hardware storage devices of claim 19, wherein the stimulus has an intensity of ≤10 mA, and wherein the stimulus is an asymmetric biphasic electrical pulse.

* * * * *